

We are IntechOpen, the world's leading publisher of Open Access books Built by scientists, for scientists

6,900

Open access books available

186,000

International authors and editors

200M

Downloads

Our authors are among the

154

Countries delivered to

TOP 1%

most cited scientists

12.2%

Contributors from top 500 universities



WEB OF SCIENCE™

Selection of our books indexed in the Book Citation Index
in Web of Science™ Core Collection (BKCI)

Interested in publishing with us?
Contact book.department@intechopen.com

Numbers displayed above are based on latest data collected.
For more information visit www.intechopen.com



Imaging Osteosarcoma

Ali Nawaz Khan¹, Durr-e-Sabih²,
Klaus L. Irion³, Hamdan AL-Jahdali⁴ and
Koteyar Shyam Sunder Radha Krishna¹

¹North Manchester General Hospital Manchester,

²Multan Institute of Nuclear Medicine & Radiotherapy,
Nishtar Medical College & Hospital, Multan,

³Cardiothoracic Centre, Liverpool NHS Trust,
The Royal Liverpool University Hospitals, Liverpool,

⁴Division of Pulmonology, Dept. of Medicine,
Head of Pulmonary Division, Sleep Disorders Center,
King Saud University for Health Science,
King Abdulaziz Medical City, Riyadh,

^{1,3}UK

²Pakistan

⁴Saudi Arabia

1. Introduction

The World Health Organization subdivides the histologic appearance of OS into central and surface tumors, and recognises a number of subtypes within each group [1]. OS frequently originate in the metaphysis of the distal femur, proximal tibia and proximal humerus. OSs are subdivided into the classic form (75%) and osteosarcoma variants (25%) [2, 3 & 4]. The variants form a heterogeneous group with a range of different imaging and behavioral features (Figures 1-7).

The long-term survival has improved thanks to more accurate diagnosis and better staging by imaging. The classic OS grows in a radial manner, which invades the bony cortex forming a ball-like area of new bone formation/destruction that compresses the surrounding soft tissues/muscles effectively forming a pseudocapsule termed as the “reactive zone.” Satellite nodules invade the reactive zone. To ensure effective surgical therapy the entire abnormal bone including the reactive zone containing the satellites is resected with wide surgical margins. OS may metastasize regionally or systemically. The presence of metastasis worsens the prognosis dramatically. Tumor nodules that grow outside the reactive zone but within the same bone or across a neighbouring joint are called “skip lesions” and represent regional metastases. Lungs are the commonest site of systemic metastases. The skeleton forms the second most common site of metastatic disease but generally occur after pulmonary metastases.



Fig. 1. The illustration shows a radiograph of a right ankle in a 12-year old. He presented with vague ankle pain and a slight limp. The radiograph shows mixed lytic and osteosclerotic lower tibial metaphyseal lesion (yellow arrow). Note the subtle laminated periosteal reaction (red arrow). A surgical biopsy confirmed a classical osteogenic sarcoma.



Fig. 2. Radiograph of the lower femur shows a sclerotic lesion of the lower femoral metaphysis. An associated exuberant "sun ray" periosteal reaction (red arrows) is seen. A biopsy revealed an osteosarcoma. Note the area of sclerosis is extending into the epiphysis.



Fig. 3. The figure show radiographs from two different patients depicting a markedly osteosclerotic lesion of the upper tibia (A) and radiograph (B) from a more skeletally mature case that shows an entirely osteolytic lesions. Both lesions proved osteosarcomas on biopsy.

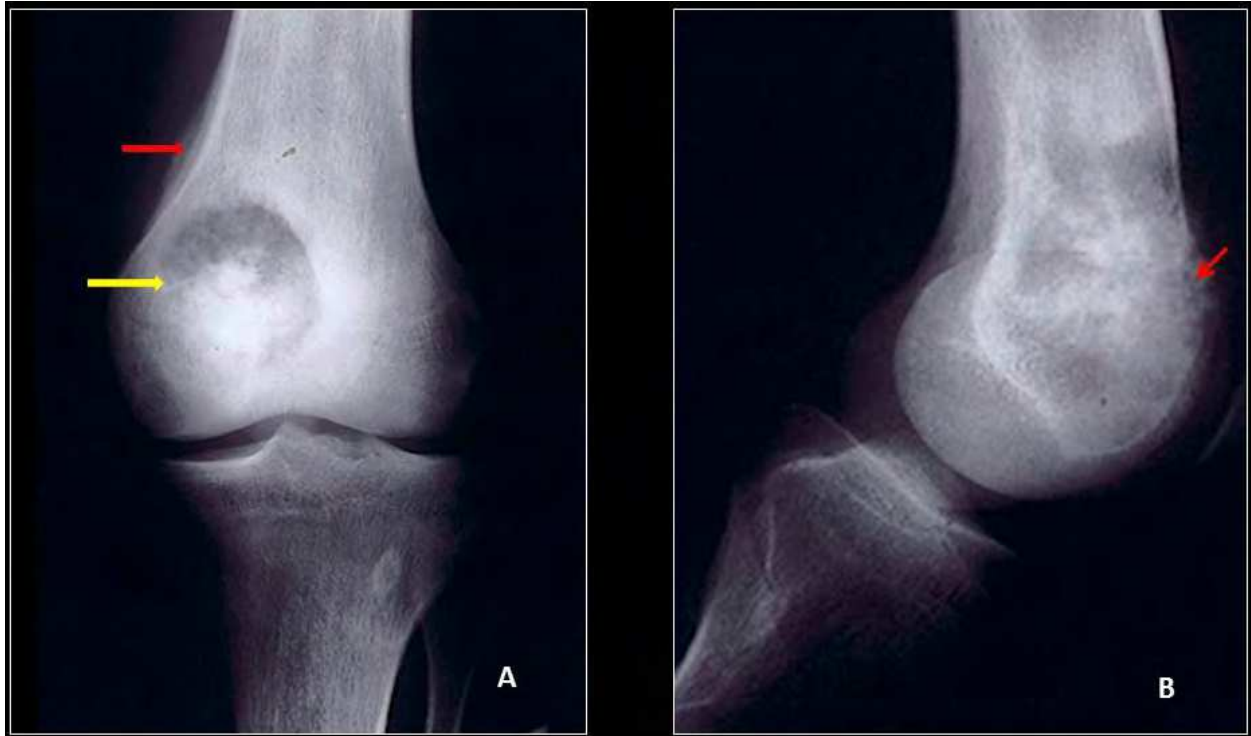


Fig. 4. The figure shows another mixed lytic and sclerotic metaphyseal tumor (yellow arrow). The tumor is crossing the epiphyseal line. Both 'sun ray' and onionskin periosteal reactions (red arrows) are shown.

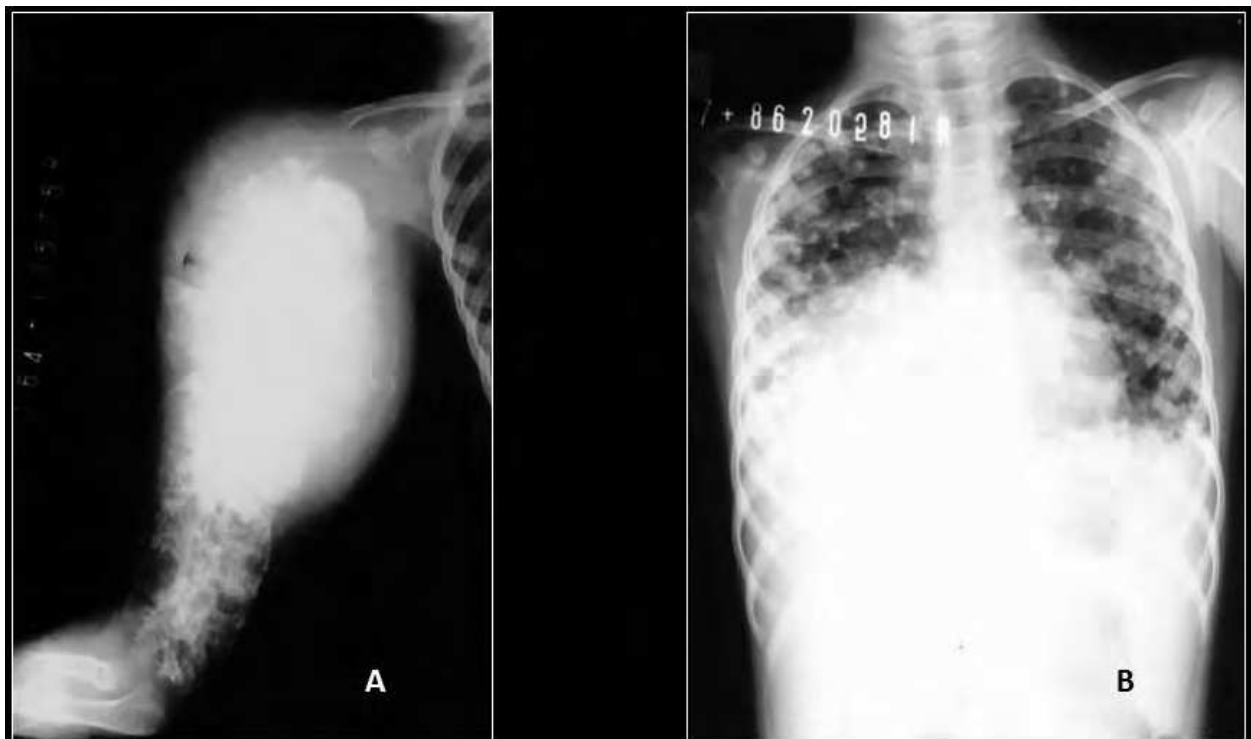


Fig. 5. Image A shows, biopsy proved osteosarcoma involving the whole shaft of the humerus. Image B depicts multiple lung metastases from the same patient. Note bilateral pleural effusions due to histologically proved pleural metastatic disease.



Fig. 6. AP and lateral radiographs of the lower femur shows a biopsy proved diaphyseal variant of OS. Note the mixed lytic/sclerotic lesion (black arrow) and the laminated periosteal new bone formation (yellow arrow).

2. Discussion

OS affects the age groups between 15–25 years in over 75% of cases with a gender ratio M:F=1.5:1. OS is uncommon in patients younger than 6 years or older than 60 years. OS in the older age group are usually secondary to Paget's disease, radiation or dedifferentiated chondrosarcomas. By far the highest percentage of OS (80% to 90%) occurs in the long tubular bones. The axial skeleton is rarely involved. Femur, tibia and humerus account for about 85% of extremity tumors. OS usually originate in the metaphysis of the long bones; tumors originating in the diaphysis and the epiphysis are rare Figures (1-7) [5 & 6].

The cause is not known but ionising radiation is implicated in 2% of OSs [7]. A genetic relationship exists with hereditary retinoblastoma. In patients with retinoblastoma, OS occurs 500 times more often than in the general population [8]. Three to four per cent children suffering from OS carry an inherent germline mutation in p53. The majority of children with germline p53 mutations have a family history suggestive of Li-Fraumeni syndrome Rarely OS is associated with single or multiple osteochondroma, solitary

enchondroma or enchondromatosis, multiple hereditary exostoses, fibrous dysplasia, chronic osteomyelitis, sites of bone infarcts, sites of metallic prostheses and sites of previous internal fixation. Ionizing radiation is a well-documented etiologic factor. OS is also associated with the use of intravenous radium and Thorotrast and exposure to alkylating agents independent of the administration of radiotherapy (Figures 8-16) [9].



Fig. 7. Image A and B shows radiographs of the lower femur in two different patients. Both represent variants of OS. Image A shows a classic OS originating at the metaphysis and invading the diaphysis. Image B is from 18-year old female shows a tumor based at the lower femoral diaphysis sparing the metaphysis. Note the exuberant periosteal reaction. The diagnosis of image B was parosteal OS.

Patients typically present with pain and swelling, localized enlargement of the extremity and, occasionally, a pathologic fracture. Most patients have localized disease at presentation. Diagnosis and treatment of OS requires a multidisciplinary approach involving the primary health care physician, radiologist, pathologist, orthopedic surgeon/oncologist, and the medical oncologist. Imaging is crucial to early diagnosis. Imaging also can predict prognosis and allows separation from other focal bone pathology. Conventional radiography is usually the primary imaging used which often provides a clue to the diagnosis and often is a guide as to which modality should follow. Once the issue of an OS is raised, MRI is the critical next step in the local staging and the associated soft tissue involvement. CT scanning is less sensitive than MRI in local staging but is essential in depicting systemic metastases specifically to the lungs. Histologic confirmation is essential, and CT is often used as a guide to obtain tumor tissue. Conventional radiography generally depicts a combination of lytic and sclerotic areas within the tumor but purely lytic or sclerotic lesions may occur. The tumor appears moth eaten, with ill-defined margins, and may appear permeative with

several small cortical erosions. The tumor near joints is often difficult to distinguish from joint effusions. Periosteal new bone formation usually occurs once the cortex is breached. Periosteal new bone formation may take a variety of shapes and forms including a Codman triangle, an onionskin appearance or hair on end/ and sunburst reactions, all indicate an aggressive process. Other imaging studies that contribute to the diagnosis and management include radionuclide studies, PET/CT and US. PET/CT holds a promise. Presently angiography is rarely used in the diagnosis of OSs except for specific indications. Bone OSs whatever the type are initially imaged by conventional radiography. Radiographs of the involved bone are obtained in various planes and often a chest radiograph is obtained in the same sitting. Once the diagnosis is suspected, MRI forms the next imaging modality of choice to assess the extent of the tumor distribution within the bone and associated soft tissue component if any. If MRI is not available, CT provides the same information though is not as sensitive. Nevertheless, CT is an essential part of a staging procedure especially in the staging of pulmonary metastases. Histological opinion is always required because of radiological mimics of OSs (Figure 17). Biopsy should always be performed before a base line MRI is obtained.

The various modalities are discussed in detail, and examples of different imaging are shown.

2.1 Stages of osteosarcoma

Staging of OSs is surgical based on Musculoskeletal Tumour Society staging system [10]:

Tumor grade (I = low grade; II = high grade);

Tumor extension (A = intraosseous involvement only; B = intra- and extraosseous extension);

Presence of distant metastases (III)

Nevertheless, imaging is required for correct staging including an isotope bone scan to rule out bone metastases and a chest radiograph and CT to rule out pulmonary metastases.

Differential diagnosis of OS includes many benign and malignant lesions and soft tissue tumors adjacent to bones particularly long tubular bones. Imaging studies alone, however, may be sometimes confusing and histological opinion is always required. Osteolytic osteosarcoma may mimic malignant fibrous histiocytoma, fibrosarcoma or giant cell tumors. The diaphyseal variant of OS may resemble Ewing's sarcoma or lymphoma [11].

Technetium-99m (^{99m}Tc) methylene diphosphonate (MDP) radionuclide bone scans are extremely sensitive but has a low specificity for OS. Nevertheless, MDP scans are useful in depicting multifocal bone disease.

Other imaging studies that contribute to the diagnosis and management include radionuclide studies, PET/CT and ultrasound. PET/CT holds a promise. Angiography is no longer used in the diagnosis of osteosarcomas.

Although ultrasonography (US) is not considered when staging OS but it is a valuable modality in tissue sampling. US is also useful in patients with prosthetic implants in the detection of early local recurrence as MRI and CT may not be suitable, because of the artifact produced by the metal on CT scans or MRIs.

3. Conventional radiograph

Conventional radiography is a non-invasive, affordable and widely available means that often provides a clue to the initial diagnosis, aggressiveness of the tumor and hence prognosis and provides a summary differential diagnosis. It can evaluate the effects of chemotherapy and diagnose lung metastases. In a suspected bone lesion, conventional radiographs are usually the initial imaging procedure. Conventional radiography may confirm a bony lesion, suggest diagnosis and guide further imaging. The anatomical location of the bone lesion the age of the patient and the clinical presentation help to formulate the list of differential diagnosis.

In a review of 347 patients with extremity OS plain-film radiographic patterns of American Joint Committee on Cancer (AJCC) stage II OA were analysed and were found to be related with clinicopathological features. The study concluded that this finding has a potential use to provide valuable information for treatment decision-making in high-grade extremity OS [12].

OS present with a variety of radiographic findings. Most OSs presents as a combination of osteolytic and osteosclerotic areas but lesions may be entirely lytic or sclerotic. Most OSs appears aggressive tumors with a moth eaten appearance and indistinct edges. Some OSs appears permeative, associated with multiple small cortical holes. Periosteal new bone formation surrounding the tumor is a common occurrence and occurs when the tumor breaks through the cortex. A Codman triangle is created when a triangular area of new subperiosteal bone formation raises the periosteum away from the bone. The main causes for this sign are OS, Ewing's sarcoma, and a subperiosteal abscess. Other types of periosteal reactions are multilaminated ("onionskin"), spiculated, and sunburst appearance ("hair on end"), all of which represent an aggressive process. Extension of the tumor beyond the bone into the surrounding soft tissues is common. As most OSs are near joints, differentiation of soft tissue extension may sometimes be difficult to distinguish from a joint effusion on radiography. 'Cloudlike' areas of sclerosis, resulting from malignant osteoid production and calcification, may be seen within the mass. Lung metastases are depicted as cannon ball lesions, which may calcify/ossify (Figures 1-7).

Following chemotherapy, OSs becomes well defined often with a surrounding 'capsule'. Atypical features in OS present diagnostic problems. Most OSs present late with aggressive features highly suggestive of OSs. However, early detection may cause diagnostic issues and tumors may be mistaken for benign lesions [13]. In these circumstances cross sectional imaging may indicate aggressive features suggestive of OS [14]. Rarely an expanding type of tumor may be, confined to the intramedullary cavity with no apparent aggressive features. Osteosclerotic OS confined to the intramedullary cavity have been confused with avascular necrosis [14, 15]. An OS may resemble an osteoblastoma or osteoid osteoma as a lytic defect with calcification or ossification within the defect and surrounded by sclerosis [14, 16].

Intracortical OS is a rare variant, which, is contained within the cortex. Radiographs may indicate a fibrous cortical defect or a Brodie's abscess. A CT scan depicts the tumor in an intra-cortical location [14, 17].

A subchondral OS originates in the subchondral position extending across the epiphyseal plate into the metaphysis. This variant may resemble a giant cell tumor or a chondrosarcoma. These variants may be entirely lytic or sclerotic. The sclerotic type has a more malignant look [14, 18].

Diaphyseal OS located in the diaphysis are radiologically similar to classical OS. Rarely, diaphyseal OS may have a more sclerotic appearance resembling a benign process. A lytic tumor with or without multilaminated periosteal reaction may resemble Ewing's sarcoma [14, 19].

Cavariar OS are a rare variant that comprise less than 2% of all OSs [20]. The radiographic appearance is similar to classic OS. Lytic appearance is more common, but periosteal reaction is rare but a sclerotic hair on end appearance may indicate a poor prognosis. Most calvarial OS occur in young adults but a secondary type of OS occurs in the fifth decade or beyond and usually is associated with Paget's disease and radiation therapy [14].

Osteosarcoma of the calcaneus occurs in less than 1% of the cases. Radiographic findings are similar to the classic OS. There is a rare association with Rothmund-Thompson syndrome [14].

OS complicating Paget's is rare but well recognized with incidence of 0.95%. Paget's related OS primarily affect males in the seventh decade of life (Figure 8-11). The distribution of lesions is similar to that expected with uncomplicated Paget's disease. The sites most commonly affected sites are the pelvis, femur and humerus. The bones of the pelvis are most commonly involved; the humerus and the femur are next in frequency. No region of the skeleton is spared, with the exception of the forearms and hands. In 30 per cent of cases, these neoplasms are multifocal. The tumors are categorized radiographically as lytic, mixed, and sclerotic, in descending order of frequency. Diagnosis on plain radiographs may be quite difficult because of the underlying Paget's changes and osteolytic lesions that sometimes occur in Paget's disease. Histologically these tumors are typically highly polymorphic sarcomas. The prognosis is poor with only 3%-8% of patients surviving at five years. The main cause of death is pulmonary metastasis or local extension of tumor growth. A high index of suspicion should be maintained when evaluating radiographs of patients with Paget disease, especially of those who present with pain or a palpable mass [21, 22 & 23].



Fig. 8. Two images of the mid shaft of the femur that shows a pathological fracture. The fracture occurred in a Pagetic bone. Note the heavy periosteal reaction at the fracture site (arrows). The initial diagnosis was periosteal new bone formation around a fracture site. However, a biopsy was taken that revealed a sarcomatous transformation of Paget's disease.



Fig. 9. Radiograph of a pelvis shows considerable sclerosis and coarsening of the trabecular pattern suggestive of Paget's disease. The diagnosis of Paget's disease was confirmed on previous imaging and blood biochemistry 10 years earlier. The patient had bone pain for some time but had recently worsened and had become more focal to the left hip. Note bilateral Paget's coxopathy and much more prominent sclerosis admixed with lysis in the left iliac bone. There is a soft tissue component superior to the left hip. Because of the atypical symptoms a radiographic changes a biopsy was taken. The biopsy confirmed sarcomatous transformation of Paget's disease.

There is a rare association of OS and a bone infarct. Imaging diagnosis may be difficult with such a relationship as changes seen suggest benign characteristics of a bone infarct. Diagnosis only become apparent with advanced OS. In a review of 50 cases of infarct associated OS, a disproportionate number of patients were black. In most patients, there was no known cause for the infarct, whereas in the remainder, the most common underlying disease was a earlier dysbaric event or alcoholism. Approximately 75% of the patients had multiple bone infarcts. Most infarct associated OS involved the femur, tibia, humerus and the radius in that border of frequency. The survival rate in patients with infarct-associated OS is poor [24, 25].

The main limitations of plain radiography in OS are underestimation of the tumor's extent within and outside of the bone and other bone lesions, such as Ewing sarcoma, chondrosarcoma, and fibrosarcoma, infections or Langerhans cell histiocytosis may resemble OS on plain radiographs [26].

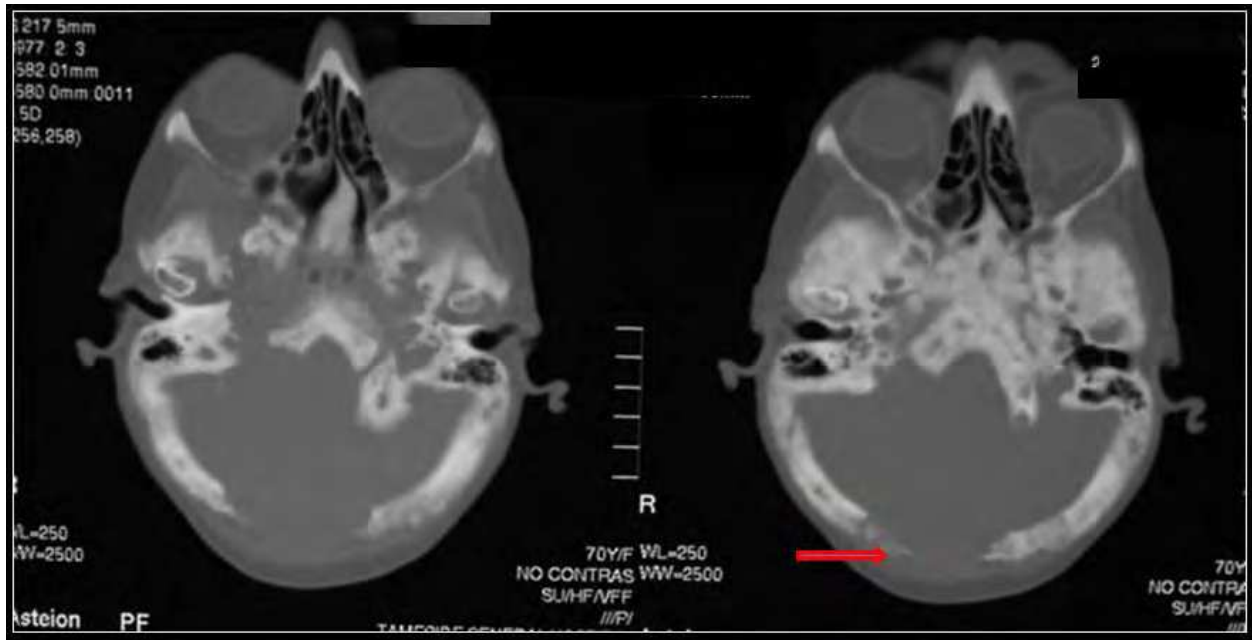


Fig. 10. Non-contrast CT scans performed on the skull of a 70-year old female known to have Paget’s disease. The patient had recently presented with increasingly severe occipital headaches. The scans show dense sclerosis at the base of the skull in keeping with Paget’s disease. Note the area of bone destruction of the occiput (arrow). The CT scans show the usefulness of the technique in the presence complex bone structure. A biopsy taken from the occipital bone revealed a sarcomatous transformation of Paget’s disease.



Fig. 11. MRI scans on the same patient as in Figure 10 depicted in T1W and Gadolinium enhanced axial, coronal and sagittal images. The images show an enhancing occipital skull diploic mass that is sparing the brain (see Figures 10).

4. Magnetic resonance imaging

MRI is the modality of choice in the evaluation of focal benign and malignant bone lesions. MRI has excellent capabilities in the local staging of malignant tumors because of its good bone marrow and soft tissue contrast and multiplanar facility. As calcium returns no signal, MRI is insensitive to small foci of calcification. Not only does MRI makes a significant contribution to correct local staging of OS it also assists in determining the most appropriate surgical management. The most fundamental purposes of local staging, is the assessment of tumor relationship of the anatomic domain from which it originates. MRI fulfills this job exceptionally well and defines individual bones, joints, and surrounding fascia and neurovascular bundles elegantly. Ultimate prognosis of OS depends on the number of compartments involved (Figures 13, 14 & 21-23, 25-26, 28) [27, 28, 29, 30 & 31].



Fig. 12. Thumb and hand radiographs from the departmental archives of two unrelated patients. Patient A had suffered from a solitary enchondroma of the first metacarpal bone for some time. The radiograph shows an expansile lytic lesion in the first metacarpal bone. A histological diagnosis of OS was made. Image B is from a patient that had worked with radium watch dials 20 years earlier. The image shows a biopsy proved OS of the first metacarpal bone. Note the mixed lytic/sclerotic lesion of the first metacarpal bone, also note the periosteal reaction and surrounding soft tissue swelling.



IntechOpen

Fig. 13. AP and lateral radiographs of the lower femur of 76 year old man that had suffered from chronic osteomyelitis for some years. The patient recently presented with a change in the pattern of symptoms. The images show destruction of the lower femur associated with periosteal new bone formation. Some of the destroyed bone is well corticated indicative of a chronic process. Initial diagnosis was that of recrudescence of osteomyelitis. The patient was treated accordingly despite a negative aspiration. A repeat radiograph (see next image) show worsening “sun ray” periosteal that prompted a biopsy, which showed OS complicating chronic osteomyelitis.



Fig. 14. AP and lateral radiographs of the lower femur of 76 year old man that had suffered from chronic osteomyelitis for some years. The patient recently presented with a change in the pattern of symptoms. The images show destruction of the lower femur associated with periosteal new bone formation. Some of the destroyed bone is well corticated indicative of a chronic process. Initial diagnosis was that of recrudescence of osteomyelitis. The patient was treated accordingly despite a negative aspiration. A repeat radiograph (see previous image) show worsening “sun ray” periosteal that prompted a biopsy, which showed OS complicating chronic osteomyelitis (also see Figure 13).

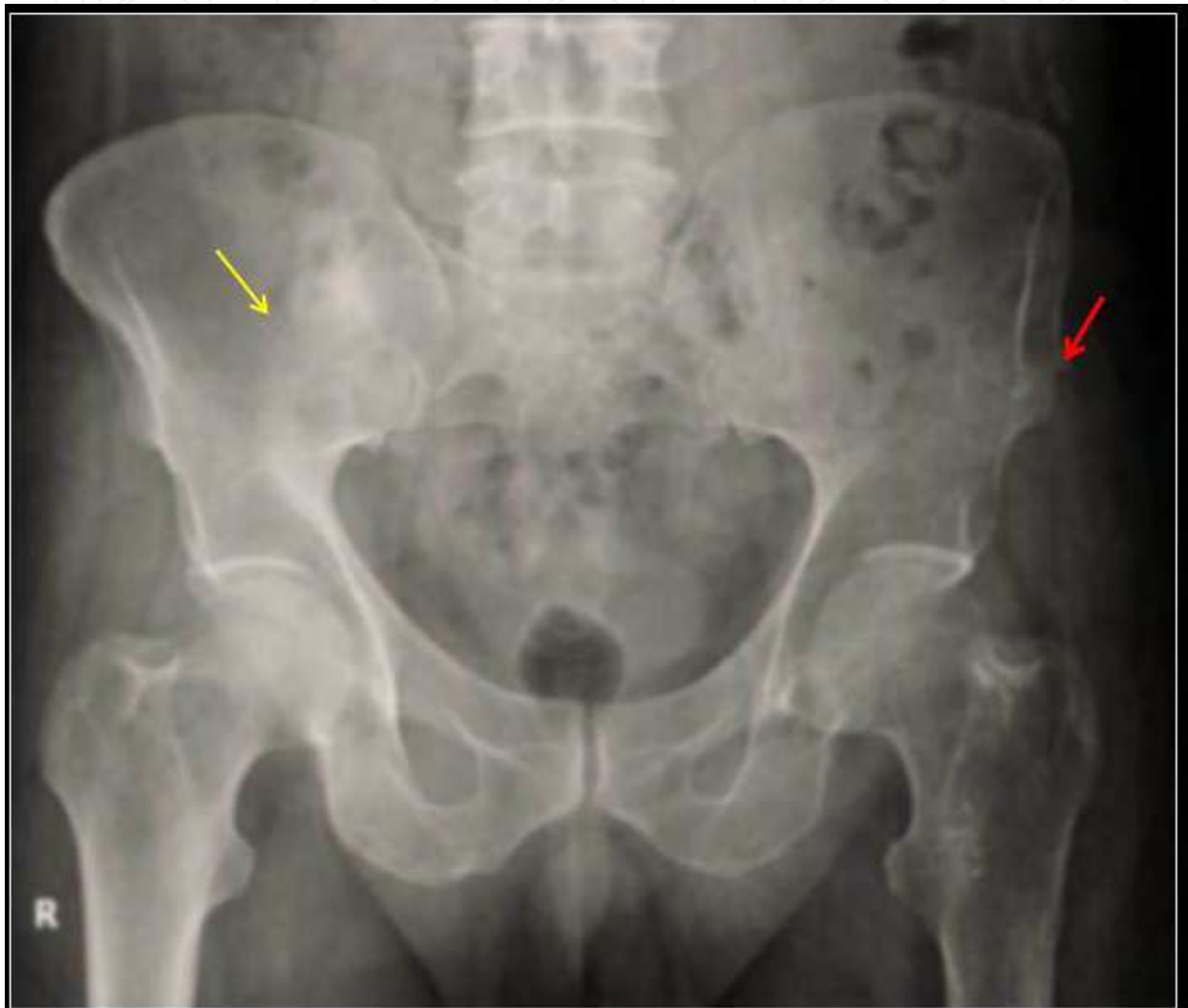


Fig. 15. An AP radiograph of pelvis from a patient with known multiple hereditary exostoses that presented with a 3 month history of increasing right buttock pain. There is a mixed lytic/osteosclerotic lesion in the right iliac bone adjacent to the right sacroiliac joint. A biopsy was taken, which showed a sarcomatous degeneration. An exostosis is noted arising from the region of the left anterior super iliac spine.

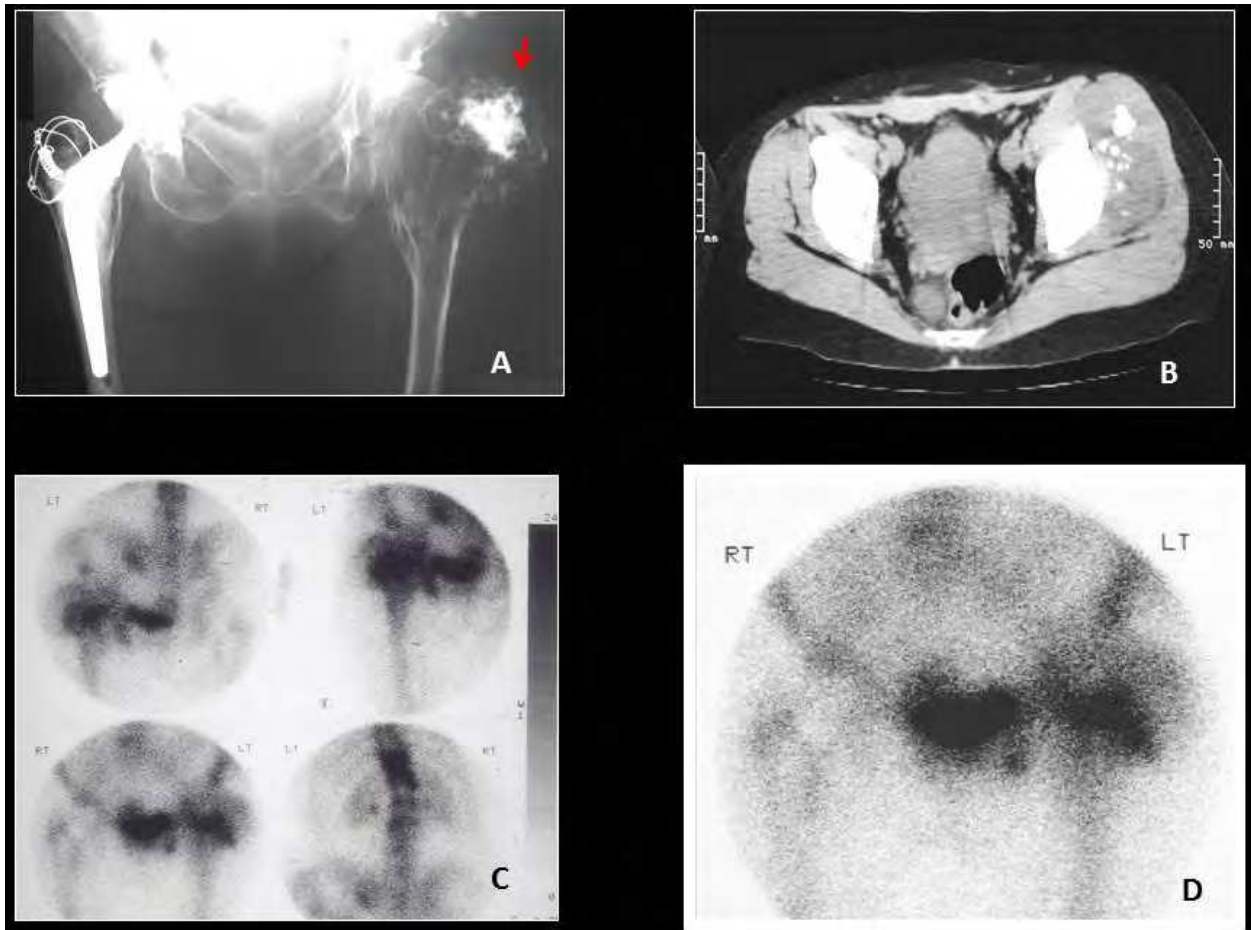


Fig. 16. Series of images from a patient with a long and family history of multiple hereditary exostoses are shown above. The patient presented with increasing pain over the left greater trochanter. An exostosis of the left greater trochanter was recorded 4 years earlier on radiograph taken prior to a right hip replacement. Image B is from an un-enhanced axial CT through the trochanter. The section shows calcification overlying the left greater trochanter associated with overlying prominent soft tissues. This finding by itself does not represent a malignant change. Images C and D show technetium-99m (^{99m}Tc) methylene diphosphonate scans. The MDP scans show intense activity in the region of the left greater trochanter and L1/L2 vertebral bodies. A biopsy taken from the greater trochanter confirmed OS. The activity in L1/L2 were subsequently proved secondary to osteoporotic fractures.



Fig. 17. Imaging studies may be sometimes confusing. Purely osteolytic osteosarcoma may mimic malignant fibrous histiocytoma, fibrosarcoma or giant cell tumours. Osteosarcoma with diaphyseal location may suggest Ewing's sarcoma or lymphoma. Occasionally traumatic periostitis/traumatic myositis ossificans may resemble OS as in this case.



Fig. 18. A radiograph of the left knee of a 65-year old man is shown. The radiographic appearances are characteristically those of an OS. Figures 19-26 are images from the same patient showing the value of various modalities.



Fig. 19. A chest radiograph of the patient from figure 18 showing calcified cannon ball lung metastases.

IntechOpen



Fig. 20. A technetium-99m (^{99m}Tc) methylene diphosphonate scan was performed on the same patient as in Figure 18 to look for other bone lesions. Activity is seen in the left lower femur associated intense hyperemic peritumoral isotope uptake.



Fig. 21. Unenhanced CT scan through the upper left femur, which shows a break in the cortex (arrow) associated with cortical thinning and effacement of intramedullary bone marrow. The described observations are at a much higher level than depicted by radiography and the MDP scan. It is difficult to be certain as to whether these findings are related to reactive bone changes or a skip lesion as no biopsy was taken from this focus. Nevertheless the CT scan demonstrate its potential.

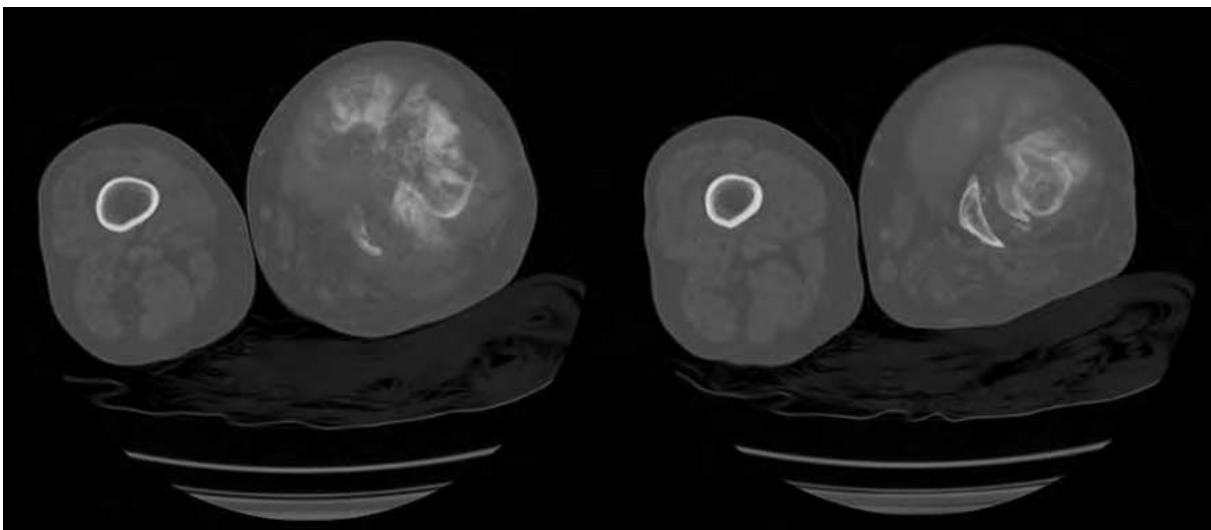


Fig. 22. Axial CT scans (the same patient as in Figure 18) through the lower left femoral tumor showing a mixture of osteosclerotic and lytic changes associated with 'sun ray' periosteal new bone formation. Also, seen are surrounding muscle and subcutaneous edema.

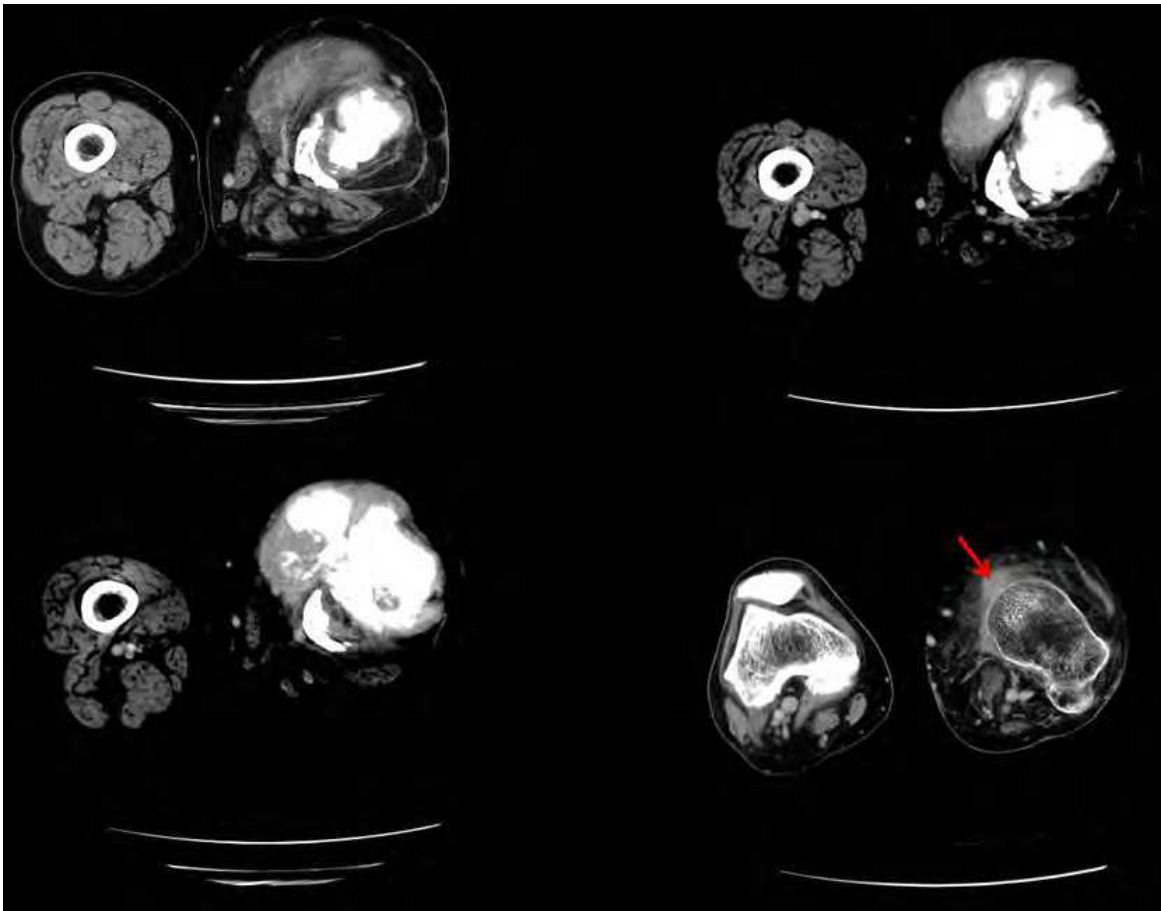


Fig. 23. Axial CT scans (the same patient as in Figure 18) through the lower left femoral tumor showing a mixture of osteosclerotic and lytic changes associated with 'sun ray' periosteal new bone formation. The images are interpreted on a soft tissue window. The images show growth of the tumor into the knee joint (arrow).

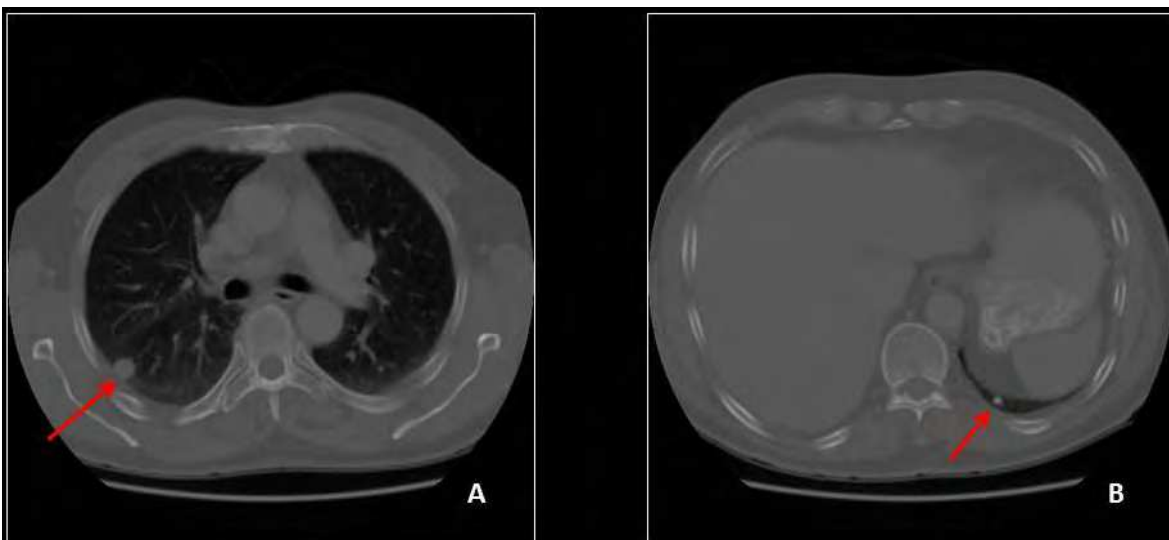


Fig. 24. Axial CT scans (same patient as in Figure 18) through the lungs interrogated on a bone window showing lung metastases. The lesion in the left costophrenic angle (image B) is calcified/ossified.

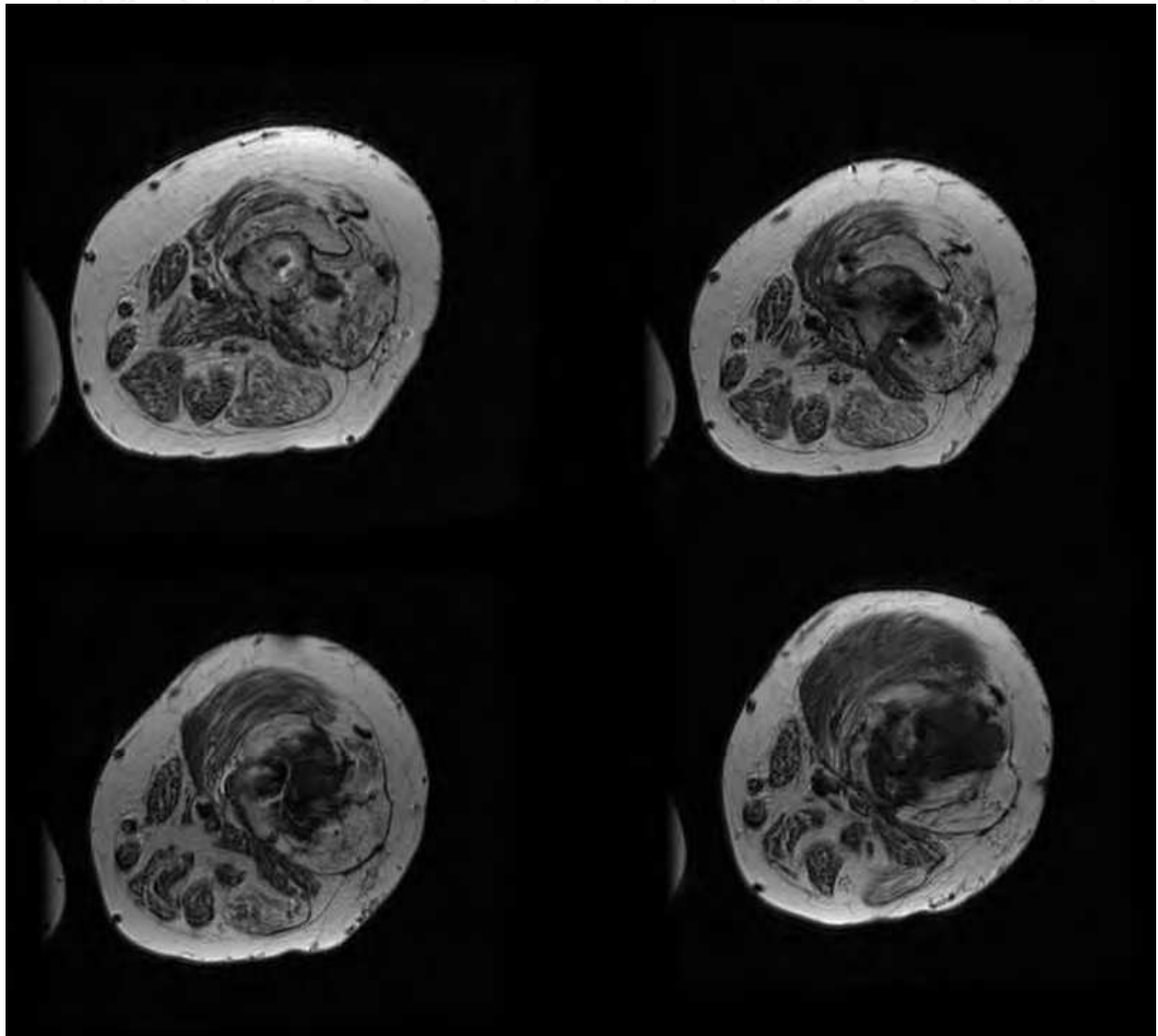


Fig. 25. Axial T1W MRI scans through the tumor (same patient as in Figure 18) showing low signal osteosclerotic bone lesion.

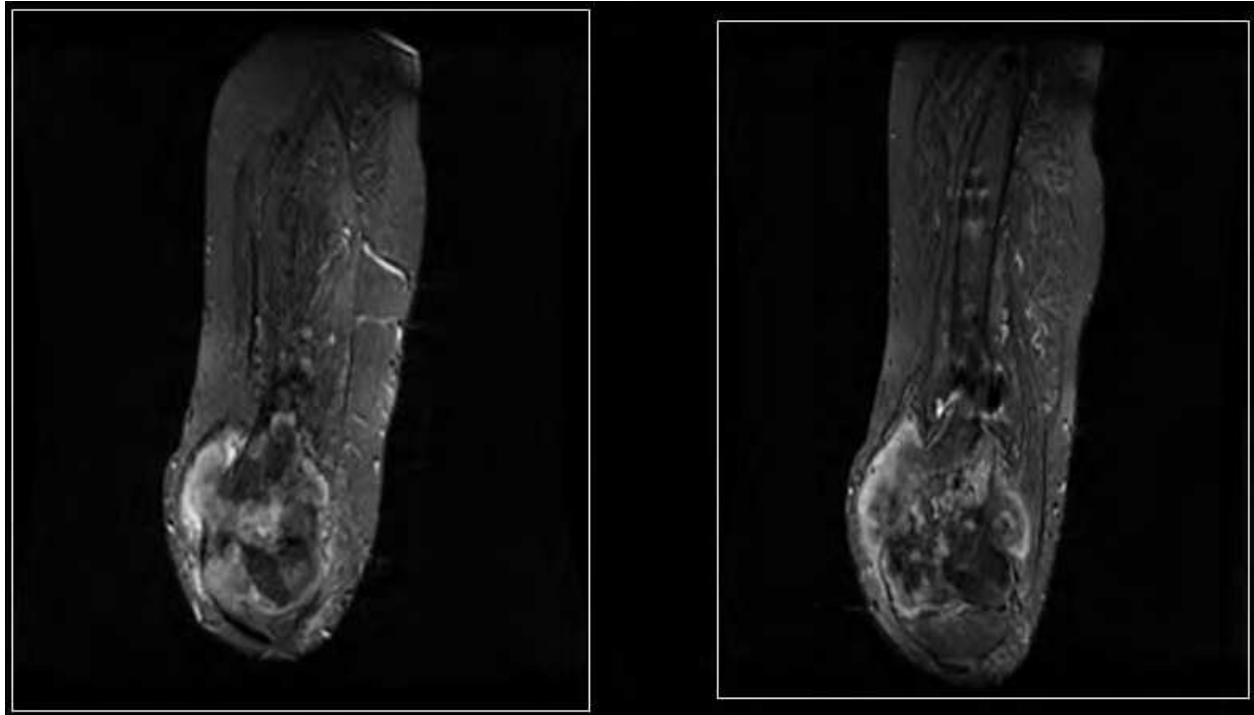


Fig. 26. STIR sequence coronal images (same patient as in Figure 18) show the extent of the tumor and tissue edema.

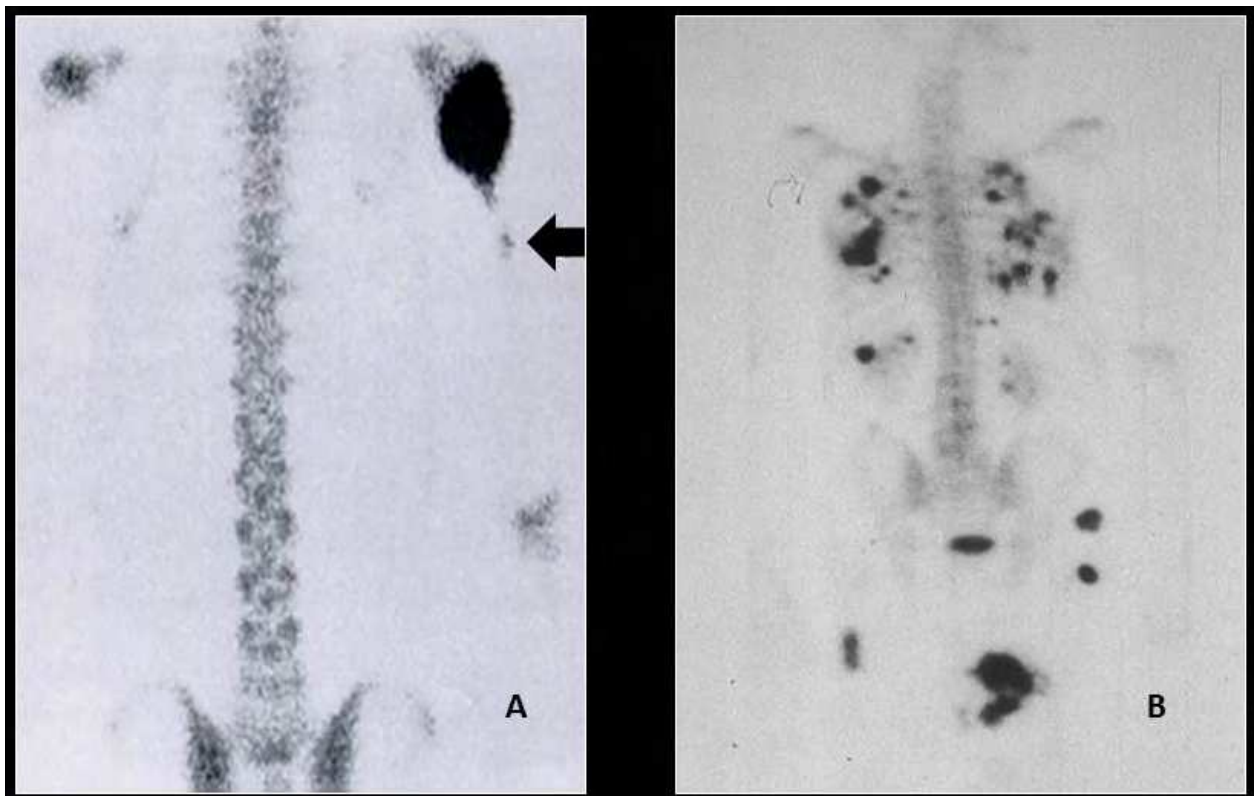


Fig. 27. Two images from technetium-99m (99m Tc) methylene diphosphonate bone scans are shown to demonstrate the importance of this technique in the diagnosis of OS. Image A show a skip lesion in OS (arrow). Image B shows extensive bony metastases from OS.

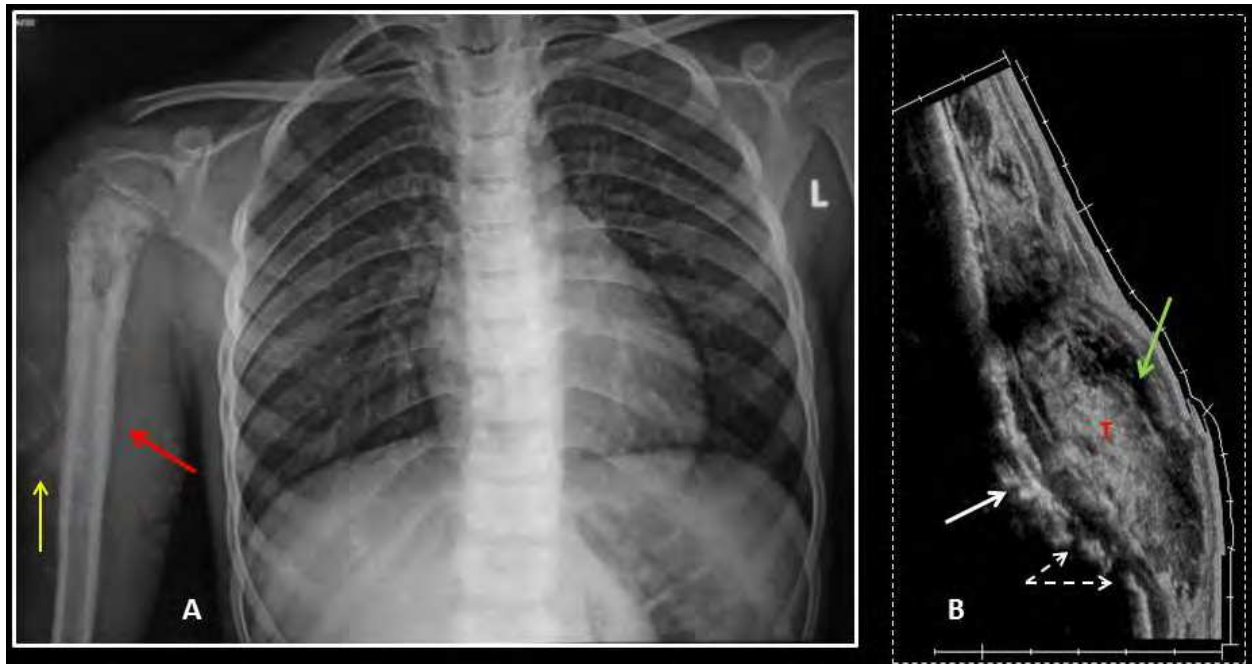


Fig. 28. A chest radiograph of a 13 year old boy showing a destructive lesion of the metaphysis and upper third of the shaft of the right humerus. The image shows a permeative lesion with surrounding periosteal reaction (red arrow) and a Codman triangle (yellow arrow). The child presented with pain in his right shoulder following minor trauma. Image B shows a longitudinal ultrasound examination of the right humerus. The image shows the tumor itself (T) periosteal new bone formation (white arrow) edema surrounding the tumor (green arrow) and a hole in the cortex (interrupted arrows). The areas pinpointed by the interrupted arrows would lend itself to a guided biopsy.

When assessing solitary bone lesions either a T1-weighted or a short-tau inversion recovery (STIR) sequence should be performed to include the entire bone.

The inclusion of the whole length of the bone is necessary to image skip lesions and evaluate the longitudinal distance of the tumor. The epiphysis is also included. Accurate assessment of the extent of intraosseous and extra osseous extension of the tumor is a crucial parameter that will ultimately affect the treatment and prognosis. Periosteal OS is of chondroblastic origin and present with high signal on T2W MRI [29, 32].

Histological opinion is required in suspected OS. Biopsy should be performed following MRI evaluation as hemorrhage occurring at the biopsy site alters the signal intensity characteristics of the tumor at subsequent MRI examinations [28].

T1W spin-echo MR images provide the most accurate estimate of the longitudinal extent of the tumor. STIR sequence overestimates the extent of the tumor because of edema and marrow hyperplasia, which may show signal changes similar to the tumor. It is necessary to determine the maximum longitudinal extent of the tumor, and its maximal distance from the articular surface of the nearest joint.

Epiphyseal tumor growth is associated with signal changes within the epiphysis similar to the tumor and may be seen in association with focal destruction of the growth plate. Both

STIR and T1-weighted sequences are correct in the diagnosis of epiphyseal tumor growth, and although T1W MR is more specific, STIR sequence images are slightly more sensitive.

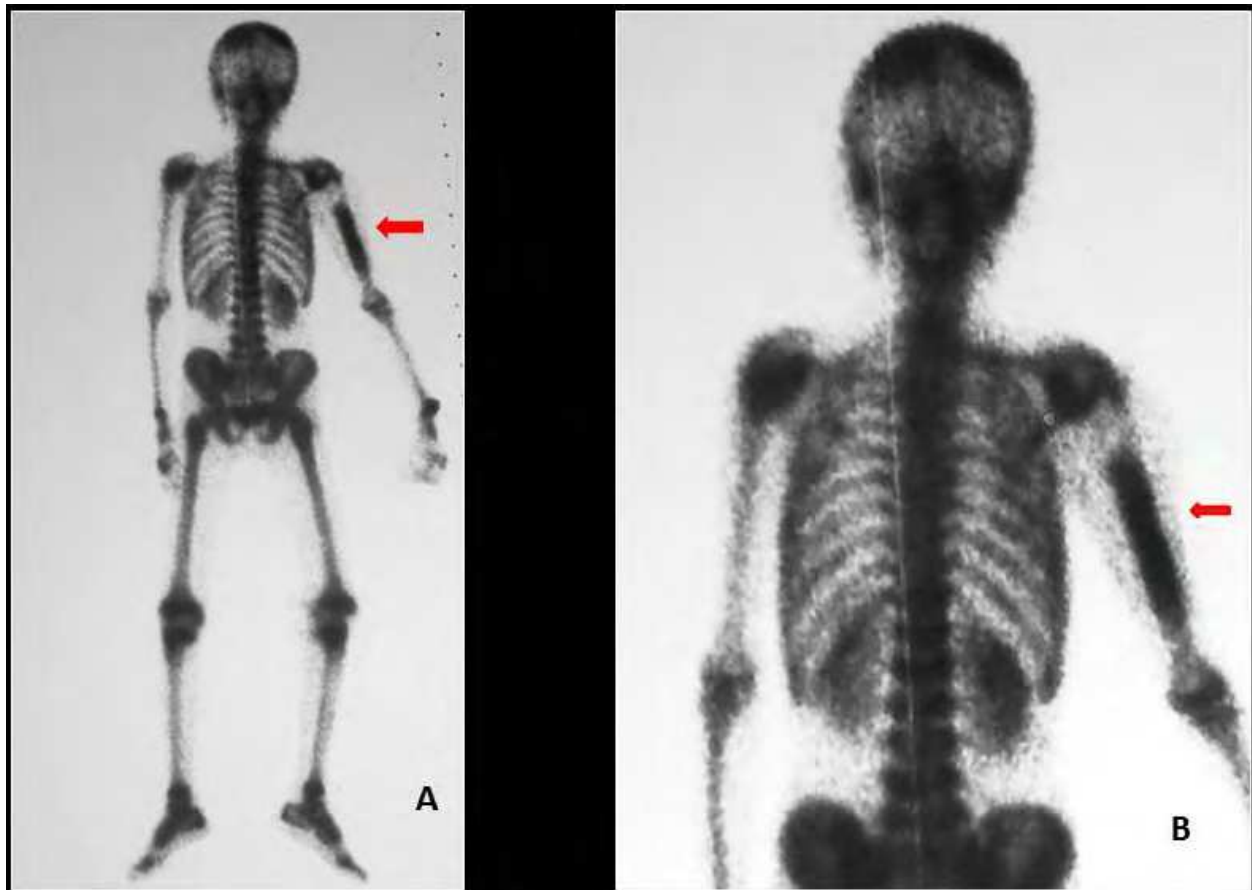


Fig. 29. An MDP bone scan on the same child as in Figure 28 shows a single lesion right humerus (arrow) B is a magnified of A. Note that the metaphysis is relatively photon deficient. Excessive osteoclastic activity may explain the reduced isotope uptake in the upper humerus.

Skip lesions associated with OS are foci of tumor quite distinct and at a distance from the primary tumor represent metastases. Tumor deposits across a joint but on the ipsilateral side are termed transarticular skip metastases. Patients with skip lesions have a more guarded prognosis and are more likely to have distant metastatic disease and shorter periods of disease-free survival.

The extent of extraosseous tumor element and its relationship to the muscle compartment and the neurovascular bundles and adjacent joints is well depicted on STIR and fat-suppressed, T2-weighted or proton density-weighted sequences. The neurovascular bundle is regarded as disease free when an intervening plane of muscle or fat is seen separating the tumor from the neurovascular bundle. When the tissue plane between the tumor and the neurovascular bundle is abolished, disease extension is presumed. Tumor extension to a joint is assumed when tumor tissue is seen within the joint breaching the subarticular bone and cartilage. Tumor infiltration along the cruciate ligaments is regarded diagnostic of tumor extension into the knee joint. MRI is more accurate in identifying tumor growth to the cruciate ligaments than to the intrasynovial joint space.

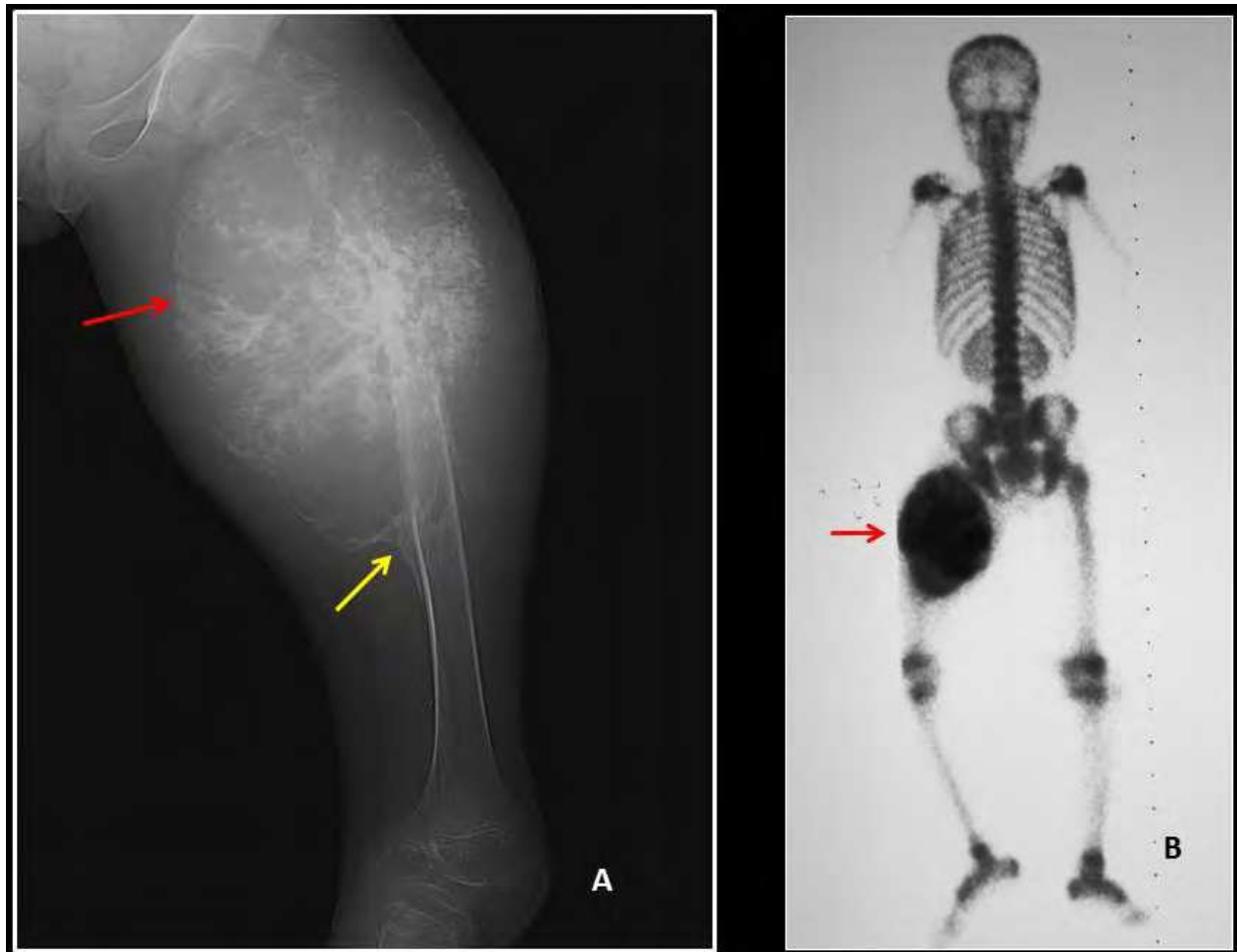


Fig. 30. This 12-year old boy presented with a painful swelling of the left upper thigh. A radiograph of the left, upper femur shows an aggressive bone lesion. There is destruction the femoral metaphysis and upper two third of the shaft of the femur. Note the exuberant periosteal 'sun ray' periosteal reaction (red arrow) and A Codman triangle (yellow arrow). Image B is an MDP scan showing intense activity at the tumor site.

Four patients with progressive pain associated with Paget's disease were evaluated with MRI. Conventional radiographs showed diffuse progressive osteolysis, cortical resorption, insufficiency fractures, bowing, and cortical and trabecular thickening. MRI showed preservation of fatty marrow signal in all phases of Paget's disease except in patients with an acute fracture and sarcoma. Small focal linear or oval areas of low signal were seen against a background of normal marrow signal on short or long TR/TE, which did not resemble a tumor. The findings suggest that unless an acute fracture or tumor is present fatty marrow signal is preserved in advanced Paget's disease [33].

MRI to confirm or exclude a sarcoma evaluated five symptomatic patients with Paget's disease. Two patients whose MRI showed a low signal' abnormality on the T1-weighted sequence corresponding to osteolysis on the radiograph were found to have malignant degeneration. Three patients with preservation of fat signal in areas of osteolysis were not biopsied and ultimately prove benign. In symptomatic patients, with Paget's disease with osteolysis but preserved marrow signal on T1-weighted MRI may be used in the basic decision-making process between conservative follow-up and biopsy [34].

Dynamic gadolinium contrast-enhanced MRI (DCE MRI) has been evaluated in a number of areas in the management of OS. The use of DCE MRI provides useful information as the characteristics of the enhancement pattern differ in viable tumor. DCE MRI has been found useful in high lighting the most appropriate location for a tissue biopsy. DCE MRI is useful in detecting joint involvement. Although MRI is highly sensitive for detecting joint invasion, false-positive diagnoses may lead to over staging of tumor and result in unnecessarily radical surgical procedures [35]. 'High signal' intensity on T2W MRI is not reliable in predicting the Grade of parosteal OS. Contrast enhanced T1-weighted images can be valuable to show the solid component in the heterogeneous areas on T2-weighted images, and can be useful in guiding a biopsy [36].

Gd-enhanced MR imaging could assist in obtaining diagnostic biopsy material of chondroblastic OS by identifying both osteoid and chondroid forming tissues. Geirnaerdts MJ et al found that septonodular and peripheral rim enhancement represented tumor with a pure chondroid matrix, whilst non-enhancing and heterogeneous enhancing areas represented tumor with both chondroid and osteoid matrix [36, 37].

Yakushiji et al found diffusion weighted MRI (DWI) more reliable than DCE MRI in differentiating between chondroblastic osteosarcoma and chondrosarcoma or other types of osteosarcoma [38].

In order to detect differences in MRI between chondroblastic osteosarcomas (CO) and the other types of osteosarcomas or chondrosarcomas (CS) using gadolinium-enhanced versus diffusion-weighted sequences Yakushiji T et al recruited 5 CO, 17 other types of OS and 18 CS. Both CO and CS showed a similar enhancement pattern; both showed septonodular and peripheral rim enhancement. The authors found DWI more useful for differentiating between CO, OS and CS or other types of osteosarcoma than Gd-enhanced MRI [38].

MRI can evaluate treatment response to chemotherapy. Oka et al evaluated the role of Diffusion-weighted MRI in 22 patients with OS, before and after chemotherapy, using the average and minimum apparent diffusion coefficient (ADC). The authors found the minimum ADC a better tool than the average apparent diffusion coefficient ADC for evaluating the chemotherapeutic response of patients with osteosarcoma. Conventional and diffusion-weighted MRI can predict chemotherapeutic response of OS early in the disease course, and it correlates well with necrosis. In addition, newly derived parameter diffusion per unit volume appears to be a sensitive substitute for response evaluation in OS [39, 40].

Gadolinium based contrast has been linked to nephrogenic systemic fibrosis. The use of contrast requires intravenous access and adds extra cost and time to the procedure. Although it may have a role in the staging of OS, its use is not universally accepted and many centers do not currently consider it a standard part of the staging protocol.

5. Computed tomography

CT and MRI are the imaging procedures of choice in locoregional staging as either modality depicts intraosseous and extraosseous spread, skip metastases, growth plate and articular involvement. Thoracic CT is the study of choice in detecting lung metastases [26, 41].

CT is particularly advantageous in clarifying OS in areas with difficult bone structure, such as the maxilla, mandible or pelvis where inconsistent images are seen by conventional

radiography. In this setting, CT scans provide a clearer picture of regional anatomy, bone destruction, as well as the extent of soft tissue mass, the nature and extent of parosteal, periosteal, and surface high-grade OS.

CT scanning may render small amounts of mineralized osseous matrix not seen on radiographs and thus alter the differential diagnosis. CT is especially useful, in visualizing flat bones where periosteal changes may be more difficult to recognize.

CT is useful in the evaluation of some OS variants. Telangiectatic osteosarcoma may be confused with an aneurysmal bone cyst especially when associated with fluid/fluid levels. A contrast-enhanced CT scan can be useful in discriminating such a lesion from an aneurysmal bone cyst. Telangiectatic OS is often associated with dense nodular tissue and matrix mineralization at CT in a largely hemorrhagic and/or necrotic osseous lesion with an associated soft-tissue mass, a feature that allows differentiation from aneurysmal bone cyst [42]. The nodular tissue surrounding telangiectatic OS is made up of tumor cells that surround the cystic spaces. This tissue rim shows typically nodular enhancement after the intravenous administration of contrast material.

Periosteal OS and high-grade surface OS may have similar plain film findings. However, histologic and radiological findings are considered together to provide a definitive diagnosis. Prognosis is dictated by tumor size and histologic grade. CT and MRI are more accurate than other imaging for preoperative diagnosis of tumor extent and for assessing tumor relationships to the bone cortex and medullary cavity (Figures 21-26) [43].

A CT guided needle biopsy is a safe and effective technique that is pertinent in the diagnosis and management of musculoskeletal tumours [44, 45].

CT ideally investigates the exclusion of metastatic OS. Lung nodules discovered on CT are biopsied or resected. Solitary nodules represent pseudometastasis in about 25% of cases [46]. Pseudo-metastases should always be confirmed in patients with OS. Some advocate that even if the nodules disappear following chemotherapy, the patient should undergo a thoracotomy. Small foci of residual cancer may occur, and they will most probably reappear in the original CT-positive areas if the patients do not have a thoracotomy and removal of nodules. Calcified/ossified tumors within the lungs have a broad differential diagnosis (see Table 1).

6. Nuclear medicine

OS typically show increased uptake of radioisotope on bone scans obtained by use of technetium-99m (^{99m}Tc) methylene diphosphonate (MDP). The uptake is dependent on the amount of osteoblastic activity within the tumor. The bone uptake is often more than the extent of the tumor due to reactive response surrounding the tumor. The size of the tumor is therefore, difficult to assess on bone scans. Skip lesions and pulmonary metastases may also pick up the radioisotope, but skip lesions are more reliably depicted by MRI. Bone scans are most useful in excluding multifocal disease. The sensitivity of bone scans in the diagnosis of OS is high, but specificity, is low as a multitude of bone lesions show increased isotope uptake including trauma, metabolic bone disease, tumors and infections (Figure 27, 29-30).

Multiple-gated acquisition (MUGA) cardiac scans are often required to monitor the harmful effects of certain chemotherapy, and a baseline line scan is often obtained.

(99m)Tc-MIBI scintigraphy can be used to assess response to chemotherapy in OS. (99m)Tc-MIBI scintigraphy has been compared with (201) Tl scintigraphy, angiography, and conclusions drawn that it could effectively predict the final response to chemotherapy of OS [47].

Increased Tc-99m MDP uptake has been reported in sarcomatous degeneration in a patient with Paget's disease. As expected Tc-99m MDP imaging showed abnormal uptake in both Paget's and the sarcomatous change. However, Tl-201 imaging showed increased uptake in the sarcomatous lesion only. The finding supports the idea that Tl-201 scintigraphy may have a potential role to play in the differentiation of Paget's disease from malignancy [48].

Positron emission tomography (PET) provides physiological understanding of both normal and abnormal body tissues. PET scanning uses a wide range of radiotracers some tissue specific. The most widely used radiotracer is an analogue of glucose specifically F-18 fluoro-2-deoxy-D-glucose (FDG). FDG uptake in body tissues is equivalent to the intensity of glucose metabolism, which increases many folds in malignant tissue. FDG-PET has become the criterion standard in initial staging, monitoring therapeutic response in the management of various cancers. However, the lack of anatomical information has resulted in the complex fusion imaging with CT. Thus, PET-CT not only provides physiological information, but also structural information leading to the diagnosis of sub-centimetre lesions. The detection of smaller lesions has made the procedure useful in the early diagnosis of the disease process and decreasing false-positive lesions [49]. Positron emission tomography imaging is a powerful emerging imaging technique in the management of sarcomas. Its applications include tumor grading, staging, therapy monitoring, and prognostication in both adult and pediatric populations [50]. The degree of tumor necrosis is indicative of progression-free survival, overall survival, and tumor necrosis in OS where (18) F-FDG PET/CT can be used as a prognostic indicator [51]. FDG-PET scanning depicts significant additional information in staging of pediatric sarcoma, which has a relevant impact on treatment planning when compared with other conventional imaging modalities [52]. FDG-PET/CT has a complementary role in the establishment of local recurrence and distant metastases in pediatric sarcomas [53].

The long-term survival with bone sarcomas is closely linked to the response to pre-operative chemotherapy. Response to chemotherapy is assessed in a variety of ways: Clinically, by demonstrating a reduction in pain and swelling of the affected limb. Imaging features of a positive response are a reduction in tumor vascularity and edema on CT or MRI. Conventional radiography is not a reliable indicator of increased vascularity or edema. However, radiologic findings have limitations. The actual size of OS show no change after chemotherapy, and it is difficult to estimate bone response objectively. Therefore, responders can be difficult to distinguish from non-responders by CT or MRI. The histologic response is considered the most reliable prognostic indicator for survival of patients with OS. However, the histologic response can only be obtained after surgery, which might not always be available in inoperable tumors. FDG-PET can be used as a non-invasive surrogate to predict response to chemotherapy in children with bone tumors [54].

7. Ultrasound

Presently there are no advantages of ultrasound over other imaging techniques and ultrasound has not been widely accepted in the diagnosis of OS, but there are certain

exceptions where US excels. The US features of bone neoplasia include bone destruction, elevated periosteum and a soft tissue mass. Giant cell tumors, malignant bone tumors, bone cysts, as well as metastatic lesions, have differing sonographic features with one study showing that sonography has equally high accuracy in the diagnosis of these tumors compared with conventional radiography (Figure 28 & 31) [55].

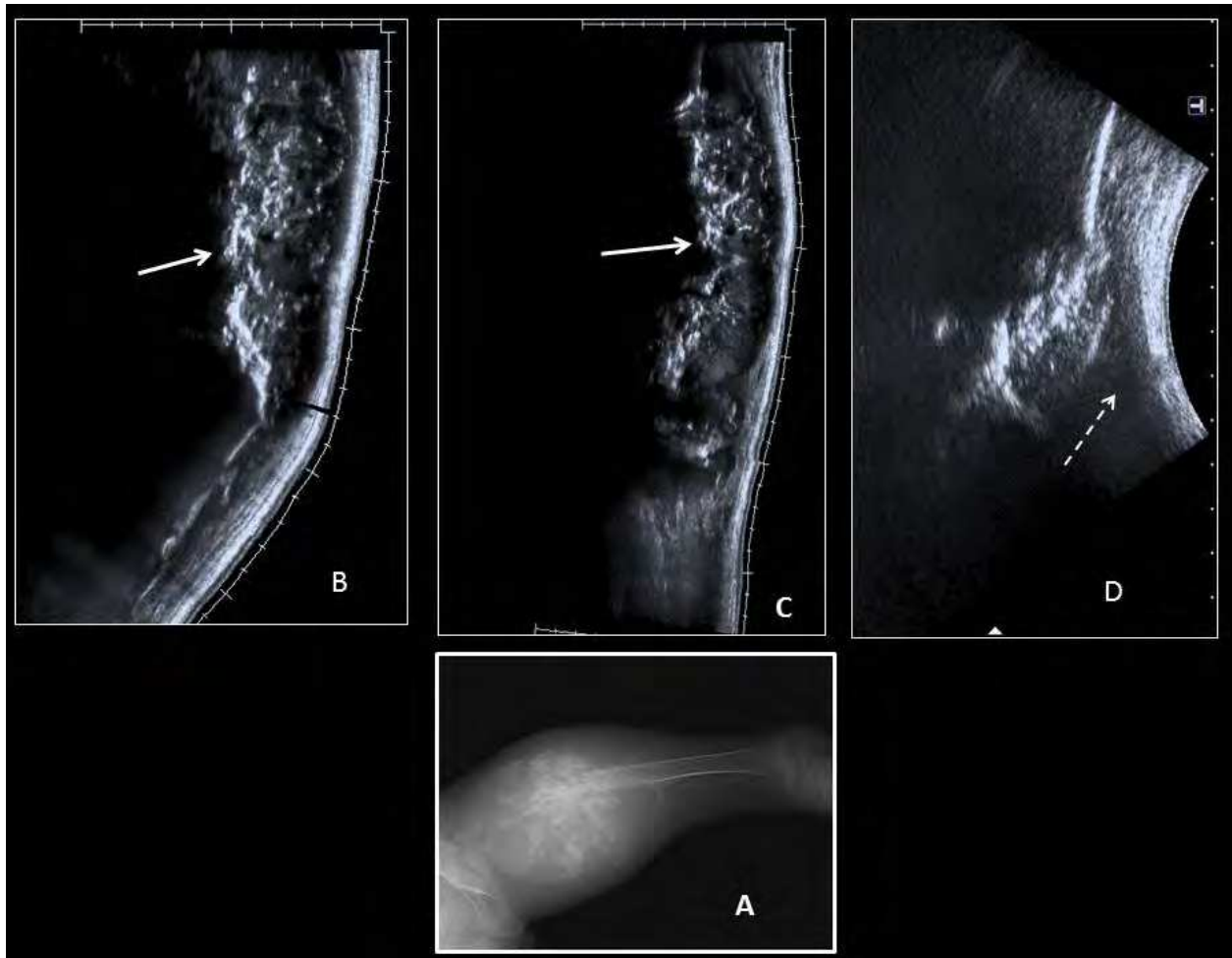


Fig. 31. Ultrasound images of the femur of the same patient as in Figure 33. Note the periosteal reaction (A & B) and a soft tissue window, which can be used for obtaining tissue for biopsy purposes.

Ultrasound features of an OS of the mandible have been described in a young adult. The patient presented with a facial swelling, and an infected lower third molar tooth that was extracted. Subtle signs were missed on dental radiographs. However, an ultrasound examination was crucial in identifying signs of malignancy including a soft tissue mass associated with bone thinning, erosion, expansion, and the "sunray" appearance of the buccal cortex, which were reminiscent of OS. Subsequently other imaging confirmed these findings [56].

Wild et al studied five patients with histologically confirmed OS by US and colour Doppler US. The features included a large soft tissue tumor with echogenic osteosclerotic areas and echo-free caverns within the tumor. Cortical destruction and periosteal elevations were well

depicted. Compared to normal tissue there was increased vascularity associated with increased blood flow in colour coded Doppler sonography in the region of the tumor. Sonography and colour coded Doppler sonography are valuable additions of conventional radiology to describe the structure, growth and blood supply of an OS [57].

Lau et al described a parosteal OS that presented 20 years following initial diagnosis, that was treated with wide excision and mega-prosthesis to reconstruct the femur. The tumor recurred in proximity to the femur prosthesis and encased half the femoral stem. Because of a metal prosthesis at the site of recurrence, US was used to detect the lesion. The tumor was eventually treated successfully, with extensive local re-excision. The case emphasise the importance of long-term follow up of parosteal sarcomas and the role of US in the presence of metal prosthesis [58].

Ultrasound is an invaluable skill for guided biopsies. OSs that have broken through the cortex into the soft tissues is receptive to US guided biopsy. Saifuddin and associates have assessed the diagnostic accuracy of US-guided Trucut needle biopsy in patients with suspected primary bone tumors. Of 144 patients, 63 were considered suitable for US-guided biopsy. The results of needle biopsy were compared with those of surgical biopsy. The diagnostic accuracy was 98.4%, with only a single failed biopsy. The authors regard US as a highly reliable method of guidance for percutaneous needle biopsy of bone tumors [59].

US can effectively evaluate the extra-osseous component of malignant and aggressive benign bone tumors arising from bone surfaces. Periosteal reaction, cortical destruction, pathological fractures, matrix mineralization, fluid-fluid levels and involvement of the neurovascular bundle are readily detected. However, ultrasound was found to be of immense help in guiding percutaneous needle biopsy [60].

Ahrar et al took, image guided biopsies on 33 patients with 35 bone lesions suspicious for OS. Of those 35 biopsies, 12 were performed fluoroscopical or with CT guidance. In 23 patients, MRI revealed a soft tissue component; in these cases, biopsies were US guided to target the soft tissue component of the tumor. All 23 US-guided biopsies resulted in positive diagnosis. Two of the 12 fluoroscopy- or CT-guided biopsies (17%) were inconclusive [61].

Soft tissue recurrence of OS may follow limb salvage surgery, and insertion of a metallic endoprosthesis, which is well depicted by US and lends itself to US guided biopsy [62].

Ultrasound has been invaluable in predicting response of OSs to chemotherapy. van der Woude et al have studied the efficacy of sequential color Doppler sonography in predicting histopathologic response to neoadjuvant chemotherapy of high-grade bone sarcomas. They concluded that a decreased or unaltered resistive index in the arteries that feed tumors, in addition to continuing, intratumoral flow and high-frequency Doppler shifts after two cycles of chemotherapy suggested a poor histologic response whilst an increased resistive index after two cycles is indicative of significant response [62]. Bramer et al used Color Doppler US in pediatric osteosarcoma and found that it can predict chemotherapy response, but not survival. The method could be useful in planning treatment prior to definitive surgery [63].

High-intensity focused ultrasound has been used in tumor ablation. Chen et al have evaluated US-guided high-intensity focused ultrasound ablation of malignant bone tumors and found it feasible and effective, and have suggested that eventually it may become a part

of limb-sparing techniques. Chen et al also concluded that sonographically guided high-intensity focused ultrasound ablation was a safe and practical method of treatment of osteosarcoma which salvages the limb, but large-scale randomized clinical trials are needed for confirmation [64, 65].

8. Radiological intervention to assist tissue diagnosis

Biopsy is always required in a suspected OS as there is a comprehensive clinical and imaging differential more over histology prognosticate the tumor. Orthopedic surgeons choose an open biopsy. However, a large core needle image guided biopsy may suffice. Recently, a fine needle aspirate (FNA) for cytological investigation has been advocated, but there is a margin of error in the interpretation of FNA as under-diagnosis or incorrect diagnosis may occur. The accuracy of FNA in primary malignant bone tumors is 86.9%, and specificity a 100%, and cytological categorization of tumors is possible in the majority of cases. This eliminates the need for bioptic confirmation [66, 67]. Material from FNA may provide additional information from electron microscopy, immunocytochemistry, cytochemistry, DNA-ploidy analysis, chromosomal analysis and molecular genetics [68]. The biopsy tract should be placed where the tract could be excised. Kilpatrick et al reviewed the clinicopathologic features of 145 FNA biopsy specimens from 140 patients without a previous diagnosis of sarcoma. Most FNA specimens are easily recognized as sarcoma, but subtyping is more accurate in bone sarcomas. Histologic subtyping of adult soft tissue sarcomas is often difficult, but this fact by itself has no impact on initial therapy. In contrast, subtyping of pediatric sarcomas by FNA seems most accurate and is essential for proper therapy [69].

Altuntas et al retrospectively studied CT guided core biopsies in a series of 127 patients with musculoskeletal tumors. The accuracy of the CT-guided core needle biopsy was determined by comparing the histology of the biopsy with the final histology of the specimen obtained at open biopsy or surgical resection of the tumor. The effective accuracy was determined, by the accuracy of the biopsy to distinguish between a benign and malignant tumor. The overall accuracy of CT guided core needle biopsy was 80.3%. The effective accuracy as determined by a malignant versus benign lesion was 89%. CT guided core needle biopsy was considered a safe and effective approach to obtain material from musculoskeletal tumors including OS [70].

Histologically differential diagnosis of OS is not immune to erroneous interpretation, as OS may have to be distinguished from a malignant fibrous histiocytoma or a poorly differentiated fibrosarcoma. Rarely an OS may histologically resemble a soft tissue sarcoma or an aneurysmal bone cyst. Therefore, when interpreting histology of bone tumors clinical and radiological correlation is vital [71, 72].

Yang et al retrospectively reviewed data from 508 image-guided needle biopsies of patients with suspected musculoskeletal tumors to determine factors leading to non-diagnostic results. The interpretations of 89% needle biopsies were correct and clinically useful. Nine per cent were non-diagnostic, and 2% were wrong. Bone lesions had a higher non-diagnostic rate than soft tissue lesions (13% vs. 4%). Rare subtypes of OS had higher incorrect rates than other diagnoses. Repeat needle or open biopsies were performed in 14% patients. Bone lesions were more likely than soft tissue lesions to require repeat biopsies. The authors concluded that a high rate of accuracy and clinical usefulness are possible with image-guided needle biopsies of musculoskeletal lesions with an experienced musculoskeletal

tumor team with regular communication to correlate clinical, radiographic, and histologic data for each patient [73].

Careful planning of the biopsy site and track must be undertaken to prevent contaminating the soft tissues that the surgeon would not otherwise remove. The biopsy track is usually resected at surgery. If delay is anticipated between biopsy and surgery, the track may be marked with suture, to facilitate eventual safe surgical resection.

9. Angiography

Angiographic findings associated with OSs include neovascularity and hypervascularity, tumor staining, early venous drainage, arterial displacement, and arterial diameter changes. Tumor staining is most familiar with osteolytic OS. These angiographic findings are not specific as similar changes occur in other malignant bone tumors. These angiographic findings are not usually seen with benign tumors with an exception of an occasional arterial displacement. The extra-skeletal part of OS is better depicted by angiography, which is not clearly seen on conventional radiography. Usually, the extra-skeletal part of OS is larger than that in giant cell tumor [74]. During the last three decades, the development of CT and MRI has determined that conventional angiography no longer be routinely performed in the diagnosis of OSs. Conventional angiography, however, is useful as an adjunct to the biopsy of parosteal OS [75]. Occasionally tumor and vessel relationship may sometimes be better depicted angiography than by CT. Hudson and associates found angiography useful in planning non-ablative resection of bone tumors because they demonstrated the relationships of the tumors to main vessels. Experience with CT indicates that it can accurately describe intra-osseous and soft-tissue extent of bone tumors. If CT does not accurately assess vascular relationships, angiography may still be required. Angiography may sometimes also assist in anticipating operative blood loss, demonstrating variants of vascular anatomy, or organization biopsy [76]. Sellier N and associates studied retrospectively 32 children with malignant bone tumors. All patients underwent conventional arteriography just before surgery. Angiography depicted distal foci of hypervascularity and venous thrombosis, not seen at CT. These findings may vary surgical treatment. Arteriography provides unparalleled characterization of large soft extension of the tumor and remains unchallenged in the assessment of venous involvement [77].

Angiography is an integral part of intra-arterial chemotherapy and embolization before limb salvage surgery in patients with OS of the lower extremity. Zhang HJ et al studied 47 patients that underwent Intra-arterial chemotherapy and embolization 3-7 days preoperatively to evaluate the effectiveness of this procedure on the degree of tumor necrosis and on the amount of blood loss during surgery. Limb salvage was achieved successfully in all cases. The percentage tumor necrosis induced by treatment ranged from 70.2% to 94.2%. The estimated blood loss during surgery, from drains in the postoperative period, and transfusion volumes were significantly lower in the studied patients as compared to the 65 patients who underwent surgery without preoperative intra-arterial chemotherapy and embolization. There is a significant reduction in the mean operative time in the embolized, group when compared to the controls [78]. Angiography has been used to assess response to combined intravenous and intra-arterial neoadjuvant chemotherapy. Cullen JW et al evaluated serial arteriography to evaluate tumor response, predict necrosis, and titrate the duration of combined intravenous and intra-arterial neoadjuvant chemotherapy

in patients with histologically proven high-grade OS or malignant fibrohistiocytoma of bone. Serial arteriography was highly sensitive and accurately predicted good responses and individualized and modified, dose-intensified neoadjuvant protocol with an excellent histologic response rate with minimal complications (Figure 32) [79].



Fig. 32. A peripheral angiogram showing its importance in the management of OS. The angiogram shows intense vascularity in the tumor (arrow). The popliteal artery is displaced medially. These findings are suggestive of OS in the appropriate clinical setting but not specific.

Imaging remains the corner stone of diagnosis, treatment and predicting prognosis in OSs. We have a high diagnostic armamentarium. Each imaging modality has its own indications and limitations. Most OSs are imaged initially by conventional radiographs followed by MRI and a biopsy, which may be image guided. CT, US, radionuclide imaging and angiography have advantages in areas and used if indicated.

Differential Diagnosis Calcified Lung Nodules

Single Large

Pulmonary hamartoma

Calcified granuloma

Primary lung cancer

Carcinoid

Intrathoracic sarcomas

Metastases: Primary sarcomas such as osteogenic, chondrosarcoma, synovial sarcomas, giant cell tumor, malignant mesenchymoma and fibrosarcoma of the breast, papillary and mucinous adenocarcinomas, and occasionally metastases from a medullary carcinoma

Calcifying fibrous pseudotumor

Intralobar pulmonary sequestration

Multiple Large Calcified Nodules

Amyloidosis

Hyalinizing granulomas

Progressive massive fibrosis

Metastatic pulmonary calcifications

Miscellaneous non-neoplastic lung tumors

Many rare non-neoplastic lesions of the lung may mimic lung calcified tumors; these include inflammatory pseudotumor (inflammatory myofibroblastic tumor), placental transmogrification of lung, alveolar microlithiasis and metastatic calcification.

Carney triad

Reference: Khan AN, Al-Jahdali HH, Allen CM, Irion KL, Al Ghanem S, Koteyar SS. The calcified lung nodule: What does it mean? *Ann Thorac Med* [serial online] 2010 [cited 2010 Apr 13];5:67-79.

10. References

- [1] Schajowicz F, Sissons HA, Sobin LH. The World Health Organization's histologic classification of bone tumors. A commentary on the second edition. *Cancer*. 1995;75:1208-1214.
- [2] Marcove RC, Mike V, Hajack JV, Levin AG, Hutter RV. Osteogenic sarcoma under the age of twenty-one. A review of one hundred and forty-five operative cases. *J Bone Joint Surg [Am]*. 1970;52:411-23.
- [3] McKenna RJ, Schwinn CP, Soonh KY, Higinbotham N. Sarcomata of osteogenic series (osteosarcoma, fibrosarcoma, chondrosarcoma, parosteal osteosarcoma, and sarcomata arising in abnormal bone): an analysis of 552 cases. *J Bone Joint Surg [Am]*. 1966;48-A:1-26.
- [4] Murphey MD, Robbin MR, McRae GA, et al. The many faces of osteosarcoma. *Radiographics*. Sep-Oct 1997;17(5):1205-31. [Medline].
- [5] Ottaviani G, Jaffe N. The epidemiology of osteosarcoma. *Cancer Treat Res*. 2009;152:3-13. Review.
- [6] Wolden SL, Alektiar KM. Sarcomas across the age spectrum. *Semin Radiat Oncol*. 2010 Jan;20(1):45-51. Review
- [7] Finkel MP, Reilly CA, Jr, Biskis BO. Pathogenesis of radiation and virus-induced bone tumors. *Recent Results Cancer Res*. 1976:92-103.[PubMed]
- [8] Swaney JJ. Familial osteogenic sarcoma. *Clin Orthop Relat Res*. 1973:64-68. doi: 10.1097/00003086-197311000-00010.[PubMed] [Cross Ref]
- [9] McIntyre JF, Smith-Sorensen B, Friend SH, Kassell J, Borresen AL, Yan YX, Russo C, Sato J, Barbier N, Miser J. Germline mutations of the p53 tumor suppressor gene in children with osteosarcoma. *J Clin Oncol*. 1994;12:925-930.[PubMed]
- [10] Wolf RE, Enneking WF. The staging and surgery of musculoskeletal neoplasms. *Orthop Clin North Am*. 1996;27:473-481.[PubMed]
- [11] Mirra JM. *Bone Tumors: Clinical, Radiologic and Pathologic Correlations*. Philadelphia, Lea & Febiger; 1989. pp. 248-316.
- [12] Kim MS, Lee SY, Cho WH, Song WS, Koh JS, Lee JA, Yoo JY, Jung ST, Jeon DG. Relationships between plain-film radiographic patterns and clinicopathologic variables in AJCC stage II osteosarcoma. *Skeletal Radiol*. 2008 Nov;37(11):997-1001. Epub 2008 Jul 12.
- [13] de Santos LA, Edeiken BS. Subtle early osteosarcoma. *Skeletal Radiol* 1985;13(1):44-8.
- [14] Rosenberg ZS, Lev S, Schmahmann S, Steiner GC, Beltran J, Present D. Osteosarcoma: subtle, rare, and misleading plain film features. *AJR Am J Roentgenol*. 1995 Nov;165(5):1209-14.
- [15] Campanacci M, Cervellati G. Osteosarcoma: A review of 345 cases. *Ital J Orthop Traumatol*. 1975 Apr;1(1):5-22.
- [16] Bertoni F, Unni KK, McLeod RA, Dahlin DC. Osteosarcoma resembling osteoblastoma. *Cancer*. 1985 Jan 15;55(2):416-26.
- [17] Vigorita VJ, Jones JK, Ghelman B, Marcove RC. Intracortical osteosarcoma. *Am J Surg Pathol*. 1984 Jan;8(1):65-71.
- [18] Tsuneyoshi M, Dorfman HD. Epiphyseal osteosarcoma: distinguishing features from clear cell chondrosarcoma. *Hum Pathol*. 1987 Jun;18(6):644-51

- [19] Haworth JM, Watt I, Park WM, Roylance J. Diaphyseal osteosarcoma. *Br J Radiol.* 1981 Nov;54(647):932-8.
- [20] Huvos AG, Sundaresan N, Bretsky SS, Butler A. Osteogenic sarcoma of the skull. A clinicopathologic study of 19 patients. *Cancer.* 1985 Sep 1;56(5):1214-21.
- [21] Giunti A, Laus M. Sarcoma in Paget's disease (11 cases). *Ital J Orthop Traumatol.* 1979 Dec;5(3):311-20.
- [22] Wick MR, Siegal GP, Unni KK, McLeod RA, Greditzer HG 3rd. Sarcomas of bone complicating osteitis deformans (Paget's disease): fifty years' experience. *Am J Surg Pathol.* 1981 Jan;5(1):47-59.
- [23] Greditzer HG 3rd, McLeod RA, Unni KK, Beabout JW. Bone sarcomas in Paget disease. *Radiology.* 1983 Feb;146(2):327-33.
- [24] Torres FX, Kyriakos M. Bone infarct-associated osteosarcoma. *Cancer.* 1992 Nov 15;70(10):2418-30. Review
- [25] Desai P, Perino G, Present D, Steiner GC. Sarcoma in association with bone infarcts. Report of five cases. *Arch Pathol Lab Med.* 1996 May;120(5):482-9
- [26] Spina V, Montanari N, Romagnoli R. Malignant tumors of the osteogenic matrix. *Eur J Radiol.* 1998 May;27 Suppl 1:S98-109. Review
- [27] Panuel M, Gentet JC, Scheiner C, et al. Physeal and epiphyseal extent of primary malignant bone tumors in childhood. Correlation of preoperative MRI and the pathologic examination. *Pediatr Radiol.* 1993;23(6):421-4. [Medline].
- [28] Lang P, Honda G, Roberts T. Musculoskeletal neoplasm: perineoplastic edema versus tumor on dynamic postcontrast MR images with spatial mapping of instantaneous enhancement rates. *Radiology.* Dec 1995;197(3):831-9. [Medline].
- [29] Iwasawa T, Tanaka Y, Aida N. Microscopic intraosseous extension of osteosarcoma: assessment on dynamic contrast-enhanced MRI. *Skeletal Radiol.* Apr 1997;26(4):214-21. [Medline].
- [30] Hoffer FA, Nikanorov AY, Reddick WE. Accuracy of MR imaging for detecting epiphyseal extension of osteosarcoma. *Pediatr Radiol.* May 2000;30(5):289-98. [Medline].
- [31] Saifuddin A, Twinn P, Emanuel R. An audit of MRI for bone and soft-tissue tumours performed at referral centres. *Clin Radiol.* Jul 2000;55(7):537-41. [Medline].
- [32] Gillespy T 3rd, Manfrini M, Ruggieri P, Spanier SS, Pettersson H, Springfield DS. Staging of intraosseous extent of osteosarcoma: correlation of preoperative CT and MR imaging with pathologic macroslices. *Radiology.* 1988 Jun;167(3):765-7.
- [33] Kaufmann GA, Sundaram M, McDonald DJ. Magnetic resonance imaging in symptomatic Paget's disease. *Skeletal Radiol.* 1991;20(6):413-8.
- [34] Sundaram M, Khanna G, El-Khoury GY. T1-weighted MR imaging for distinguishing large osteolysis of Paget's disease from sarcomatous degeneration. *Skeletal Radiol.* 2001 Jul;30(7):378-83. Sundaram
- [35] Schima W, Amann G, Stiglbauer R, Windhager R, Kramer J, Nicolakis M, Farres MT, Imhof H. Preoperative staging of osteosarcoma: efficacy of MR imaging in detecting joint involvement. *AJR Am J Roentgenol.* 1994 Nov;163(5):1171-5.

- [36] Dönmez FY, Tüzün U, Başaran C, Tunaci M, Bilgiç B, Acunaş G. MRI findings in parosteal osteosarcoma: correlation with histopathology. *Diagn Interv Radiol*. 2008 Sep;14(3):142-52.
- [37] Geirnaerdt MJ, Bloem JL, van der Woude HJ, Taminiau AH, Nooy MA, Hogendoorn PC. Chondroblastic osteosarcoma: characterisation by gadolinium-enhanced MR imaging correlated with histopathology. *Skeletal Radiol*. 1998 Mar;27(3):145-53.
- [38] Yakushiji T, Oka K, Sato H, Yorimitsu S, Fujimoto T, Yamashita Y, Mizuta H. Characterization of chondroblastic osteosarcoma: gadolinium-enhanced versus diffusion-weighted MR imaging. *J Magn Reson Imaging*. 2009 Apr;29(4):895-900.
- [39] Oka K, Yakushiji T, Sato H, Hirai T, Yamashita Y, Mizuta H. The value of diffusion-weighted imaging for monitoring the chemotherapeutic response of osteosarcoma: a comparison between average apparent diffusion coefficient and minimum apparent diffusion coefficient. *Skeletal Radiol*. 2010 Feb;39(2):141-6. Epub 2009 Nov 19.
- [40] Bajpai J, Gamnagatti S, Kumar R, Sreenivas V, Sharma MC, Khan SA, Rastogi S, Malhotra A, Safaya R, Bakhshi S. Role of MRI in osteosarcoma for evaluation and prediction of chemotherapy response: correlation with histological necrosis. *Pediatr Radiol*. 2011 Apr;41(4):441-50. Epub 2010 Oct 27.
- [41] Picci P. Osteosarcoma (osteogenic sarcoma). *Orphanet J Rare Dis*. 2007 Jan 23;2:6. Review
- [42] Murphey MD, wan Jaovisidha S, Temple HT, Gannon FH, Jelinek JS, Malawer MM. Telangiectatic osteosarcoma: radiologic-pathologic comparison. *Radiology*. 2003 Nov;229(2):545-53. Epub 2003 Sep 25.
- [43] Levine E, De Smet AA, Huntrakoon M. Juxtacortical osteosarcoma: a radiologic and histologic spectrum. *Skeletal Radiol*. 1985;14(1):38-46.
- [44] Altuntas AO, Slavin J, Smith PJ, Schlict SM, Powell GJ, Ngan S, Toner G, Choong PF. Accuracy of computed tomography guided core needle biopsy of musculoskeletal tumours. *ANZ J Surg*. 2005 Apr;75(4):187-91.
- [45] Schaller RT Jr, Schaller JF, Buschmann C, Kiviat N. The usefulness of percutaneous fine-needle aspiration biopsy in infants and children. *J Pediatr Surg*. 1983 Aug;18(4):398-405.
- [46] Picci P, Vanel D, Briccoli A, Talle K, Haakenaasen U, Malaguti C, Monti C, Ferrari C, Bacci G, Saeter G, Alvegard TA. Computed tomography of pulmonary metastases from osteosarcoma: the less poor technique. A study of 51 patients with histological correlation. *Ann Oncol*. 2001;12:1601-1604. doi: 10.1023/A:1013103511633. [PubMed]
- [47] Miwa S, Shirai T, Taki J, Sumiya H, Nishida H, Hayashi K, Takeuchi A, Ooi A, Tsuchiya H. Use of (99m)Tc-MIBI scintigraphy in the evaluation of the response to chemotherapy for osteosarcoma: comparison with (201)Tl scintigraphy and angiography. *Int J Clin Oncol*. 2011 Feb 18. [Epub ahead of print]
- [48] Colarinha P, Fonseca AT, Salgado L, Vieira MR. Diagnosis of malignant change in Paget's disease by Tl-201. *Clin Nucl Med*. 1996 Apr;21(4):299-301.
- [49] Kumar R, Chauhan A, Vellimana AK, Chawla M. Role of PET/PET-CT in the management of sarcomas. *Expert Rev Anticancer Ther*. 2006 Aug;6(8):1241-50.

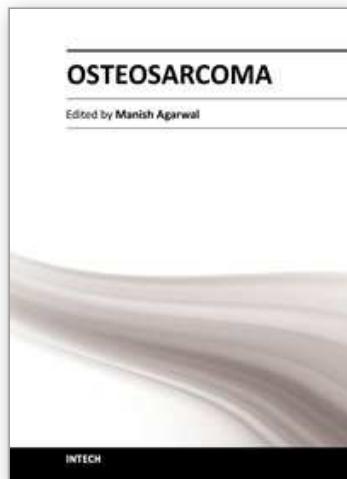
- [50] Benz MR, Tchekmedyian N, Eilber FC, Federman N, Czernin J, Tap WD. Utilization of positron emission tomography in the management of patients with sarcoma. *Curr Opin Oncol*. 2009 Jul;21(4):345-51.
- [51] Costelloe CM, Macapinlac HA, Madewell JE, Fitzgerald NE, Mawlawi OR, Rohren EM, Raymond AK, Lewis VO, Anderson PM, Bassett RL Jr, Harrell RK, Marom EM. 18F-FDG PET/CT as an indicator of progression-free and overall survival in osteosarcoma. *J Nucl Med*. 2009Mar;50(3):340-7.
- [52] Völker T, Denecke T, Steffen I, Misch D, Schönberger S, Plotkin M, Ruf J, Furth C, Stöver B, Hautzel H, Henze G, Amthauer H. Positron emission tomography for staging of pediatric sarcoma patients: results of a prospective multicenter trial. *J Clin Oncol*. 2007 Dec 1;25(34):5435-41.
- [53] Arush MW, Israel O, Postovsky S, Militianu D, Meller I, Zaidman I, Sapir AE, Bar-Shalom R. Positron emission tomography/computed tomography with 18fluoro-deoxyglucose in the detection of local recurrence and distant metastases of pediatric sarcoma. *Pediatr Blood Cancer*. 2007 Dec;49(7):901-5.
- [54] Kim DH, Kim SY, Lee HJ, Song BS, Kim DH, Cho JB, Lim JS, Lee JA. Assessment of Chemotherapy Response Using FDG-PET in Pediatric Bone Tumors: A Single Institution Experience. *Cancer Res Treat*. 2011 Sep;43(3):170-5. Epub 2011 Sep 30.
- [55] Kang B, Du J, Huang J. Sonographic diagnosis of bone tumors. *J Tongji Med Univ*. 1997;17(2):106-9.
- [56] Ng SY, Songra A, Ali N, Carter JL. Ultrasound features of osteosarcoma of the mandible--a first report. *Oral Surg Oral Med Oral Pathol Oral Radiol Endod*. 2001 Nov; 92(5):582-6.
- [57] Wild F, Erhardt J, Beck JD, Deeg KH, Stehr K. Sonographic and Doppler color sonographic findings in osteosarcoma. *Klin Padiatr*. 1991 May-Jun;203(3):155-7. [Article in German]
- [58] Lau TW, Wong JW, Yip DK, Chien EP, Shek TW, Wong LL. Local recurrence of parosteal osteosarcoma adjacent to prosthesis after 20 years: a case report. *J Orthop Surg (Hong Kong)*. 2004 Dec;12(2):263-6.
- [59] Saifuddin A, Mitchell R, Burnett SJ, Sandison A, Pringle JA. Ultrasound-guided needle biopsy of primary bone tumours. *J Bone Joint Surg Br*. 2000 Jan; 82(1):50-4.
- [60] Saifuddin A, Burnett SJ, Mitchell R. Pictorial review: ultrasonography of primary bone tumours. *Clin Radiol*. 1998 Apr; 53(4):239-46.
- [61] Ahrar K, Himmerich JU, Herzog CE, Raymond AK, Wallace MJ, Gupta S, Madoff DC, Morello FA Jr, Murthy R, McRae SE, Hicks ME. Percutaneous ultrasound-guided biopsy in the definitive diagnosis of osteosarcoma. *J Vasc Interv Radiol*. 2004 Nov; 15(11):1329-33.
- [62] Garant M, Sarazin L, Cho KH, Chhem RK. Soft-tissue recurrence of osteosarcoma: ultrasound findings. *Can Assoc Radiol J*. 1995 Aug;46(4):305-7.
- [63] van der Woude HJ, Bloem JL, van Oostayen JA, Nooy MA, Taminiau AH, Hermans J, Reynierse M, Hogendoorn PC. Treatment of high-grade bone sarcomas with neoadjuvant chemotherapy: the utility of sequential color Doppler sonography

- in predicting histopathologic response. *AJR Am J Roentgenol.* 1995 Jul;165(1):125-33.
- [64] Bramer JA, Gubler FM, Maas M, Bras H, de Kraker J, van der Eijken JW, Schaap GR. Colour Doppler ultrasound predicts chemotherapy response, but not survival in paediatric osteosarcoma. *Pediatr Radiol.* 2004 Aug;34(8):614-9. Epub 2004 May 18.
- [65] Chen W, Zhu H, Zhang L, Li K, Su H, Jin C, Zhou K, Bai J, Wu F, Wang Z. Primary bone malignancy: effective treatment with high-intensity focused ultrasound ablation. *Radiology.* 2010 Jun;255(3):967-78.
- [66] Li C, Wu P, Zhang L, Fan W, Huang J, Zhang F. Osteosarcoma: limb salvaging treatment by ultrasonographically guided high-intensity focused ultrasound. *Cancer Biol Ther.* 2009 Jun;8(12):1102-8. Epub 2009 Jun 27.
- [67] Jayaram G, Gupta M. Fine needle aspiration cytology in the diagnosis of bone tumours. *Malays J Pathol.* 1994 Dec;16(2):137-44.
- [68] Fleshman R, Mayerson J, Wakely PE Jr. Fine-needle aspiration biopsy of high-grade sarcoma: a report of 107 cases. *Cancer.* 2007 Dec 25;111(6):491-8.
- [69] Willén H. *Acta Orthop Scand Suppl.* 1997 Feb;273:47-53. Fine needle aspiration in the diagnosis of bone tumors.
- [70] Kilpatrick SE, Cappellari JO, Bos GD, Gold SH, Ward WG. Is fine-needle aspiration biopsy a practical alternative to open biopsy for the primary diagnosis of sarcoma? Experience with 140 patients. *Am J Clin Pathol.* 2001 Jan;115(1):59-68
- [71] Altuntas AO, Slavin J, Smith PJ, Schlicht SM, Powell GJ, Ngan S, Toner G, Choong PF. Accuracy of computed tomography guided core needle biopsy of musculoskeletal tumours. *ANZ J Surg.* 2005 Apr;75(4):187-91.
- [72] Campanacci M. *Bone and Soft Tissue Tumors: Clinical Features, Imaging, Pathology and Treatment.* 2. Wien, Austria: Springer-Verlag; 1999. pp. 464-491.
- [73] Mirra JM. *Bone Tumors: Clinical, Radiologic and Pathologic Correlations.* Philadelphia, Lea & Febiger; 1989. pp. 248-316.
- [74] Yang J, Frassica FJ, Fayad L, Clark DP, Weber KL. Analysis of nondiagnostic results after image-guided needle biopsies of musculoskeletal lesions. *Clin Orthop Relat Res.* 2010 Nov;468(11):3103-11. Epub 2010 Apr 10.
- [75] Hu YG. [Arteriographic findings in bone tumors: experience with 170 cases]. *Zhonghua Wai Ke Za Zhi.* 1990 Apr;28(4):195-7, 251. [Article in Chinese]
- [76] Carrasco CH. Angiography of osteosarcoma. *Hematol Oncol Clin North Am.* 1995 Jun;9(3):627-32.
- [77] Hudson TM, Enneking WF, Hawkins IF Jr. The value of angiography in planning surgical treatment of bone tumors. *Radiology.* 1981 Feb;138(2):283-92.
- [78] Sellier N, Vecchierini A, Kalifa G. [Malignant bone tumors in children. Is there still a role for arteriography?]. [Article in French] *J Radiol.* 1988 Jan;69(1):7-11.
- [79] Zhang HJ, Yang JJ, Lu JP, Lai CJ, Sheng J, Li YX, Hao Q, Zhang SM, Gupta S. Use of intra-arterial chemotherapy and embolization before limb salvage surgery for osteosarcoma of the lower extremity. *Cardiovasc Intervent Radiol.* 2009 Jul;32(4):672-8. Epub 2009 Mar 19.

- [80] Cullen JW, Jamroz BA, Stevens SL, Madsen W, Hinshaw I, Wilkins RM, Cullen P, Camozzi AB, Fink K, Peck SD, Kelly CM. The value of serial arteriography in osteosarcoma: delivery of chemotherapy, determination of therapy duration, and prediction of necrosis. *J Vasc Interv Radiol*. 2005 Aug;16(8):1107-19.

IntechOpen

IntechOpen



Osteosarcoma

Edited by Dr. Manish Agarwal

ISBN 978-953-51-0506-0

Hard cover, 174 pages

Publisher InTech

Published online 11, April, 2012

Published in print edition April, 2012

This book is aimed at quickly updating the reader on osteosarcoma, a dreaded primary bone cancer. Progress in management of osteosarcoma has been slow after the evolution of chemotherapy and limb salvage surgery. Research is now directed towards identifying molecular targets for systemic therapy. Availability of chemotherapy drugs and low cost implants in developing world have allowed limb salvage surgery to develop. This book looks at current basic knowledge on osteosarcoma and some of the developments in research which have the potential to change the prognosis.

How to reference

In order to correctly reference this scholarly work, feel free to copy and paste the following:

Ali Nawaz Khan, Durr-e-Sabih, Klaus L. Irion, Hamdan AL-Jahdali and Koteyar Shyam Sunder Radha Krishna (2012). Imaging Osteosarcoma, Osteosarcoma, Dr. Manish Agarwal (Ed.), ISBN: 978-953-51-0506-0, InTech, Available from: <http://www.intechopen.com/books/osteosarcoma/imaging-of-osteosarcoma-review>

INTECH
open science | open minds

InTech Europe

University Campus STeP Ri
Slavka Krautzeka 83/A
51000 Rijeka, Croatia
Phone: +385 (51) 770 447
Fax: +385 (51) 686 166
www.intechopen.com

InTech China

Unit 405, Office Block, Hotel Equatorial Shanghai
No.65, Yan An Road (West), Shanghai, 200040, China
中国上海市延安西路65号上海国际贵都大饭店办公楼405单元
Phone: +86-21-62489820
Fax: +86-21-62489821

© 2012 The Author(s). Licensee IntechOpen. This is an open access article distributed under the terms of the [Creative Commons Attribution 3.0 License](#), which permits unrestricted use, distribution, and reproduction in any medium, provided the original work is properly cited.

IntechOpen

IntechOpen